

## Molecular Rectification in Metal–SAM–Metal Oxide–Metal Junctions

Christian A. Nijhuis, William F. Reus, and George M. Whitesides\*

*Department of Chemistry and Chemical Biology, Harvard University,  
Cambridge, Massachusetts 02138*

Received June 15, 2009; E-mail: gwhitesides@gmwhgroup.harvard.edu

**Abstract:** This Article compares the ability of self-assembled monolayers (SAMs) of alkanethiolates with ferrocene (Fc) head groups (SC<sub>11</sub>Fc), and SAMs of alkanethiolates lacking the Fc moiety (SC<sub>10</sub>CH<sub>3</sub> and SC<sub>14</sub>CH<sub>3</sub>), to conduct charge. Ultraflat surfaces of template-stripped silver (Ag<sup>TS</sup>) supported these SAMs, and a eutectic alloy of gallium and indium (EGaIn), covered with a skin of gallium oxide (presumably Ga<sub>2</sub>O<sub>3</sub>), formed electrical top-contacts with them. EGaIn is a liquid at room temperature, but its spontaneously formed surface oxide skin gives it apparent non-Newtonian properties and allows it to be molded into conically shaped tips; these tips formed soft electrical contacts with SAMs and formed stable SAM-based tunneling junctions in high (70–90%) yields. Measurements of current density, *J*, versus applied voltage, *V*, showed that tunneling junctions composed of SAMs of SC<sub>11</sub>Fc rectify current with a rectification ratio  $R \approx 1.0 \times 10^2$  ( $R = |J(-V)|/|J(V)|$ ) at  $\pm 1$  V and with a log-standard deviation of 3.0). In contrast, junctions lacking the Fc moiety, that is, junctions composed of SAMs of SC<sub>*n*-1</sub>CH<sub>3</sub> (with *n* = 11 or 15 and presenting terminal CH<sub>3</sub> groups), showed only slight rectification ( $R = 1.5$  (1.4) and 2.1 (2.5), respectively). A statistical analysis of large numbers (*N* = 300–1000) of data gave detailed information about the spread in values and the statistical significance of the rectification ratios and demonstrated the ability of the experimental techniques described here to generate SAM-based junctions in high yield useful in physical-organic studies.

### Introduction

This Article describes a study that compares SAMs terminated in ferrocene (Fc) and methyl groups as the insulating component of the tunneling junction. The Fc-terminated junctions show high, log-normally distributed (see below) rectification ratios *R* at  $\pm 1$  V with a log-mean ( $\mu_{\log}$ ) of  $\sim 1.0 \times 10^2$ , and a log-standard deviation ( $\sigma_{\log}$ ) of 3.0 (eq 1, with *J* = current density (A/cm<sup>2</sup>) and *V* = voltage (V)). That is, 68% of the distribution of *R* lies within the range from 33 to  $3.0 \times 10^2$ , in metal–insulator–metal oxide–metal junctions.

$$R = |J(-V)|/|J(V)| \quad (1)$$

The junctions comprised self-assembled monolayers (SAMs) of 11-(ferrocenyl)-1-undecanethiol (SC<sub>11</sub>Fc) on the surface of a template-stripped silver (Ag<sup>TS</sup>) bottom-electrode, with top-contacts of eutectic indium–gallium (EGaIn 75.5%, Ga 24.5% by weight, 15.7 °C melting point) alloy. (We write this contact as Ga<sub>2</sub>O<sub>3</sub>/EGaIn to emphasize that the liquid metal alloy is covered with a semiconducting, or insulating, metal oxide film or “skin”; see below for details.) Tunneling junctions with approximately the same thickness comprising SAMs of alkanethiolates and lacking the Fc moiety, that is, SC<sub>10</sub>CH<sub>3</sub> and SC<sub>14</sub>CH<sub>3</sub>, showed much smaller rectification ratios:  $R \approx 1.5$  ( $\sigma_{\log} = 1.4$ ) and 2.1 ( $\sigma_{\log} = 2.5$ ), respectively. These values are small, but statistically significant (e.g., distinguishable from 1.0) and distinguishable from one another (see below). We performed a detailed statistical analysis to determine (i) the log-mean values of the current densities, (ii) the log-mean values of the rectification ratios, and (iii) the yield of working devices (70–90%).

In studies of tunneling across SAMs, the procedures used to determine the yields of devices, to define “working devices”, or to select “representative” devices have almost never been explicitly reported for large-area (e.g., non-scanning probe-based) junctions; the work of Lee et al.<sup>1</sup> provides a rare and welcome exception (as does the rather different system provided by break junctions by Venkataraman et al.<sup>2</sup>). To discriminate between the characteristics of the devices and artifacts, and to account for defects in the junctions (all tunneling junctions will contain SAMs that have defects due to step edges, impurities, grain boundaries, etc.),<sup>3</sup> we believe that statistically large numbers of data must be analyzed (*N* = 100–1000) and that data must not be “selected”, “filtered”, or “discarded” before undergoing statistical analysis. We emphasize that all of the data we recorded were included in our statistical analysis: no data, not even data collected for junctions that short-circuited or were unstable, were discarded prior to analysis, to avoid biasing outcomes.

Understanding the mechanisms of charge transport in organic or organometallic tunneling junctions is fundamental to the broad subject of charge transport in organic/organometallic matter and is a prerequisite for defining the potential (if any) of these junctions to provide new or improved function in devices.<sup>4</sup> Among the many types of charge transport that might

- (1) Kim, T.-W.; Wang, G.; Lee, H.; Lee, T. *Nanotechnology* **2007**, *18*, 315204.
- (2) Venkataraman, L.; Klare, J. E.; Nuckolls, C.; Hybertsen, M. S.; Steigerwald, M. L. *Nature* **2006**, *442*, 7105.
- (3) Love, J. C.; Estroff, L. A.; Kriebel, J. K.; Nuzzo, R. G.; Whitesides, G. M. *Chem. Rev.* **2005**, *105*, 1103.

be studied, rectification is especially attractive, because measurements of rectification use the same junctions to make and contrast two types of measurements (current at forward and reverse bias across the same junction; eq 1). This type of measurement minimizes some of the uncertainties and complexities of experiments that compare electrical current measurements in different junctions, because variation in current density across even carefully prepared SAM-based junctions remains significant (and in many of the systems that have been studied, this variation is so large that the data are presently uninterpretable).

Our group<sup>5</sup> and others<sup>6,7</sup> have reported molecular rectification in a variety of tunneling junctions with different molecules. These studies, as a group, have left the mechanism of rectification undefined for four reasons: (i) The reproducibility of the data has often been poor and seldom carefully characterized statistically. (The reproducibility of all SAM-based organic tunneling devices has been notoriously low, and careful and detailed studies with statistically large numbers of samples, studies necessary to establish reproducibility, have simply not been conducted. In fact, given the low yield and short lifetimes of the devices, it has been not possible to carry out such analysis.) (ii) Junctions have incorporated bottom- and top-electrodes of different materials.<sup>8,9</sup> These junctions have the potential to rectify in the absence of any structural or orbital asymmetry in the organic component. (iii) The junctions have incorporated molecules with complex structures.<sup>6,10,11</sup> Virtually no information is available concerning either the supramolecular structure of organic compounds in these junctions or the order and spectrum of defects in the SAMs. (iv) The values of the rectification ratios have been low (usually less than 10),<sup>5,6,12</sup> Given the low yields and limited reproducibility of the data in these systems in past studies, it is difficult to perform statistics on them, and we doubt that any value of the rectification ratio between 1 and 10 so far reported is interpretable. (The extensive statistical analyses included in this Article have among their several objectives that of giving us a measure of statistical confidence in the values of  $R$  between 1 and 10 that we report.)

The synthetic flexibility of our molecular rectifier, coupled with its ability to form stable, reproducible, and highly rectifying junctions with electrodes of Ag<sup>Ts</sup> and Ga<sub>2</sub>O<sub>3</sub>/EGaIn, make this system attractive for physical-organic studies whose goal is to determine a mechanism for molecular rectification. The rectification ratio is the ratio of the absolute value of the current densities at opposite bias (eq 1). Comparing opposing current densities within the same junction provides an internal standard:

the junction with current flowing in one direction provides a standard against which to compare the same junction with the current flowing in the opposite direction. This characteristic insulates  $R$  from variations encountered in comparisons of different junctions in terms of the contact area, and the quality of the contact between Ga<sub>2</sub>O<sub>3</sub>/EGaIn and the SAM, because both are the same (e.g., on the same junction) in measurements of rectification. Thus, measuring values of  $R$ , rather than values of  $J$ , may be particularly useful for systems in which the procedure used to fabricate the junctions generates junctions with uncontrolled and experimentally significant variations in contact areas, or in series electrical resistances.

## Prior Work

**Tunneling Junctions.** Most fabrication techniques for junctions have involved evaporating metals for the top contacts directly onto the SAMs.<sup>13</sup> It is now clear that these preparations have low yields (<5% when carefully done, and much lower in most studies<sup>1,14</sup>), that the evaporated metals do damage the organic molecules,<sup>15</sup> and that other phenomena (e.g., formation of metal filaments and/or metal oxides in the junctions),<sup>16–18</sup> rather than tunneling, underlie many (or most) of the current–voltage curves reported for these systems. Because many devices have incorporated complicated molecules into SAMs with no (or, perhaps, incorrect) characterization of the structures of the SAMs, it is impossible to conclude how or if the molecules inside junctions determined their electrical characteristics.<sup>19</sup>

Scanning probe techniques (SPM) have been used to contact SAMs at metal surfaces and to measure charge transport across these SAMs.<sup>20</sup> Both atomic force microscopy (AFM) and scanning tunneling microscopy (STM) can image SAMs and perform measurements on well-defined locations within a SAM. Although SPM-based techniques are useful for studying charge transport across molecules, they also have generic limitations. In STM studies, a tunneling gap always exists between the SAM and the STM tip.<sup>21</sup> In AFM studies, the force applied to contact the SAMs influences the measurements in ways that are difficult to quantify.<sup>22</sup> In both STM- and AFM-based junctions, it is difficult to know the exact number of molecules included in the junctions and to define how representative a measurement of the small area sampled by the tip is.

- (4) Lindsay, S. M.; Ratner, M. A. *Adv. Mater.* **2007**, *19*, 23.
- (5) Chabinyk, M. L.; Chen, X.; Holmlin, R. E.; Jacobs, H.; Skulason, H.; Frisbie, C. D.; Mujica, V.; Ratner, M. A.; Rampi, M. A.; Whitesides, G. M. *J. Am. Chem. Soc.* **2002**, *124*, 11730.
- (6) Ng, M.-K.; Lee, D.-C.; Yu, L. *J. Am. Chem. Soc.* **2002**, *124*, 11862.
- (7) (a) Böhme, T.; Simpson, C. D.; Müllen, K.; Rabe, J. P. *Chem.-Eur. J.* **2007**, *13*, 7349. (b) Hallböök, A.-S.; Poelsema, B.; Zandvliet, H. J. W. *Solid State Commun.* **2007**, *141*, 645.
- (8) (a) Lenfant, S.; Guerin, D.; Tran Van, F.; Chevrot, C.; Palacin, S.; Bourgoign, J. P.; Bouloussa, O.; Rondelez, F.; Vuillaume, D. *J. Phys. Chem. B* **2006**, *110*, 13947. (b) Zhou, C.; Deshpande, M. R.; Reed, M. A.; Jones, L., II; Tour, J. M. *Appl. Phys. Lett.* **1997**, *71*, 611.
- (9) Lenfant, S.; Krzeminski, C.; Delerue, C.; Allan, G.; Vuillaume, D. *Nano Lett.* **2003**, *3*, 741.
- (10) Shumate, W. J.; Mattern, D. L.; Jaiswal, A.; Dixon, D. A.; White, T. R.; Burgess, J.; Honciuc, A.; Metzger, R. M. *J. Phys. Chem. B* **2006**, *110*, 11146.
- (11) Ashwell, G. J.; Urasinska, B.; Tyrrell, W. D. *Phys. Chem. Chem. Phys.* **2006**, *8*, 3314.
- (12) Chen, X.; Jeon, Y.-M.; Jang, J.-W.; Qin, L.; Huo, F.; Wei, W.; Mirkin, C. A. *J. Am. Chem. Soc.* **2008**, *130*, 8166.

- (13) (a) Haick, H.; Cahen, D. *Acc. Chem. Res.* **2008**, *41*, 359. (b) Chen, J.; Reed, M. A.; Rawlett, A. M.; Jones, L., II; Tour, J. M. *Science* **1999**, *286*, 1550.
- (14) Bang, G. S.; Chang, H.; Koo, J.-R.; Lee, T.; Advincula, R. C.; Lee, H. *Small* **2008**, *4*, 1399.
- (15) (a) Fisher, G. L.; Walker, A. V.; Hooper, A. E.; Tighe, T. B.; Bahnc, K. B.; Skriba, H. T.; Reinard, M. D.; Haynie, B. C.; Opila, R. L.; Winograd, N.; Allara, D. L. *J. Am. Chem. Soc.* **2002**, *124*, 5528. (b) Walker, A. V.; Tighe, T. B.; Cabarcos, O. M.; Reinard, M. D.; Haynie, B. C.; Uppili, S.; Winograd, N.; Allara, D. L. *J. Am. Chem. Soc.* **2004**, *126*, 3954.
- (16) Metzger, R. M. *Acc. Chem. Res.* **1999**, *32*, 950.
- (17) McCreery, R.; Dieringer, J.; Solak, A. O.; Snyder, B.; Nowak, A. M.; McGovern, W. R.; DuVall, S. *J. Am. Chem. Soc.* **2003**, *125*, 10748.
- (18) (a) Lau, C. N.; Stewart, D. R.; Williams, R. S.; Bockrath, M. *Nano Lett.* **2004**, *4*, 569. (b) Troisi, A.; Ratner, M. A. *Small* **2006**, *2*, 172.
- (19) Stewart, D. R.; Ohlberg, D. A. A.; Beck, P. A.; Chen, Y.; Williams, R. S.; Jeppesen, J. O.; Nielsen, K. A.; Stoddart, J. F. *Nano Lett.* **2004**, *4*, 133.
- (20) Chen, F.; Hihath, J.; Huang, Z.; Li, X.; Tao, N. *J. Annu. Rev. Phys. Chem.* **2007**, *58*, 535.
- (21) Bumm, L. A.; Arnold, J. J.; Dunbar, T. D.; Allara, D. L.; Weiss, P. S. *J. Phys. Chem. B* **1999**, *103*, 8122.
- (22) (a) Engelkes, V. B.; Beebe, J. M.; Frisbie, C. D. *J. Phys. Chem. B* **2005**, *109*, 16801. (b) Wang, G.; Kim, T.-W.; Jo, G.; Lee, T. *J. Am. Chem. Soc.* **2009**, *131*, 5980.

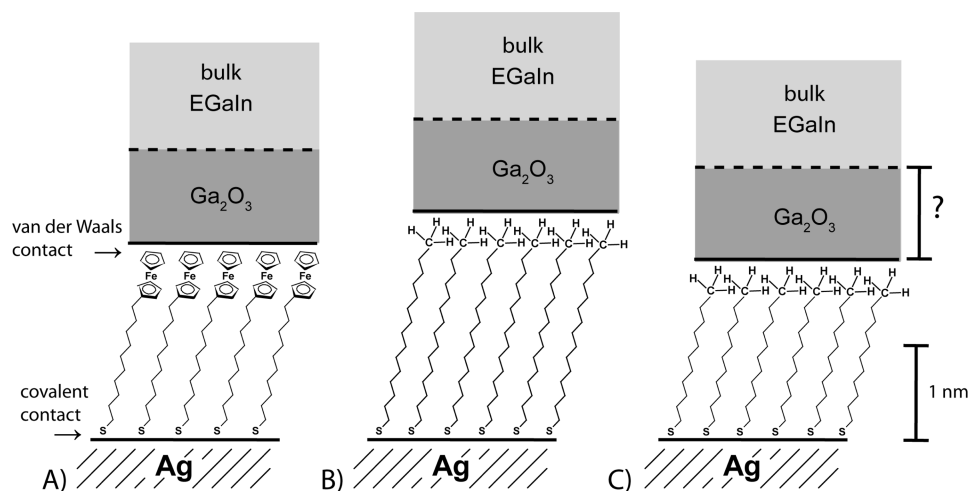


**Figure 1.** Schematic showing tunneling junctions consisting of template-stripped Ag bottom-electrodes, supporting SAMs, and contacted by Ga<sub>2</sub>O<sub>3</sub>/EGaIn. The SAMs are: (A) SC<sub>11</sub>Fc, (B) SC<sub>14</sub>CH<sub>3</sub>, and (C) SC<sub>10</sub>CH<sub>3</sub> and are drawn roughly to scale. We have not defined the thickness of the layer of Ga<sub>2</sub>O<sub>3</sub>, its exact composition, or electrical properties (see text for details).

In an important study, Akkerman et al. described a system that uses a conductive polymer (PEDOT:PSS) on top of the SAM to protect it during the deposition of metal electrodes.<sup>23</sup> This method dramatically improved the yield of working devices (to ~100%, in some cases), and these systems, where they work, are the highest yield and most stable junctions now known that incorporate SAMs. These systems also have four important ambiguities: (i) The interface of the conductive polymer with the SAM is ill-defined and depends strongly on the functional groups presented by the SAM.<sup>24</sup> (ii) These systems require an organic solvent as a minority component of the system and include a vacuum-annealing step. These characteristics of the preparation have the potential to modify the interface between the SAM and the PEDOT:PSS, and to change or damage the SAM itself, in unanticipated and unrecognized ways. (iii) The current densities in these junctions are larger than those measured by most other methods (larger by a factor of ~10<sup>3</sup> than junctions using Hg as an electrode with a SAM of equal thickness, for instance); the origin of this difference has not been established, but one possible explanation is partial dissolution of the SAM and the polymer in one another. (iv) The procedure used seems to depend strongly on the details of the molecular structure of the SAM, and apparently fails for some SAMs, for reasons that are presently obscure. Thus, although the yield and stability of these systems, when they work, make them attractive for the fabrication of devices, we are concerned that they (at their current state of development) present too many uncertainties to be a platform for fundamental, structure-based, physical and physical-organic studies.

To avoid the problems encountered with evaporating metal top-contacts, our group<sup>25</sup> and Majda,<sup>26</sup> Slowinski,<sup>27</sup> Rampi,<sup>28</sup> and others<sup>29</sup> have used Hg as a “soft” liquid–metal electrode for investigating junctions of the form Ag-SAM//SAM-Hg. It seems that these systems also require a protective layer between the SAM and the top metal: for stability, the Hg-drop electrode had to be covered with a short-chain SAM (e.g., of SC<sub>10</sub>CH<sub>3</sub>), and measurements had to be carried out in hydrocarbon solvents containing free HSC<sub>10</sub>CH<sub>3</sub>. Cahen et al. have measured tunneling junctions of single SAMs of *n*-alkanethiols immobilized on a drop of Hg in contact with Si/SiO<sub>2</sub>.<sup>29</sup> Although this procedure makes it possible to measure the tunneling characteristics across single SAMs, it also requires or uses a protective layer, which

adds a resistive or tunneling component: that is, the SiO<sub>2</sub> between the SAM and the Si bottom-electrode.

Although using Hg-SC<sub>10</sub>CH<sub>3</sub> as an electrode made it possible to characterize charge transport across SAMs using junctions with relatively large areas (0.1–1.0 mm<sup>2</sup>), yields in these junctions were typically low (~25%), and the junctions were unstable to repeatedly cycling and to aging (perhaps because Hg amalgamates with the other metals, Ag, Au, used as the bottom-electrodes).

It seemed possible that defects, topographical irregularities in the top-surface in the evaporated metal films, and thus in the Au/SAM or Ag/SAM structures, provided nucleation points that initiated failures, and we have explored the flatter electrodes produced by template stripping.<sup>30</sup> The use of Ag<sup>TS</sup> substrates, rather than substrates deposited by electron-beam evaporation, improved the yield (by a factor of 3.5) and the reproducibility of measurements carried out using the Hg-SC<sub>10</sub>CH<sub>3</sub> top-electrodes. Still, in our hands, the yield and reproducibility of this system were not satisfactory for routine use. Ga<sub>2</sub>O<sub>3</sub>/EGaIn is far less prone to alloying and short-circuiting than Hg and thus offers (i) higher yields (>80%) of working junctions in most cases, (ii) greater ease of manipulation, and (iii) more rapid collection of large amounts of data.<sup>31</sup> Also, Ga<sub>2</sub>O<sub>3</sub>/EGaIn has the advantage over Hg that is nonvolatile and nontoxic.

(23) (a) Akkerman, H. B.; de Boer, B. *J. Phys.: Condens. Matter* **2008**, *20*, 013001. (b) Akkerman, H. B.; Blom, P. W. M.; de Leeuw, D. M.; de Boer, B. *Nature* **2006**, *440*, 69.

(24) Akkerman, H. B. Large area molecular junctions. Ph.D. Thesis, University of Groningen, The Netherlands, 2008; ISBN 978-90-367-3441-7.

(25) (a) Haag, R.; Rampi, M. A.; Holmlin, R. E.; Whitesides, G. M. *J. Am. Chem. Soc.* **1999**, *121*, 7895. (b) Holmlin, R. E.; Haag, R.; Chabynyc, M. L.; Ismagilov, R. F.; Cohen, A. E.; Terfort, A.; Rampi, M. A.; Whitesides, G. M. *J. Am. Chem. Soc.* **2001**, *123*, 5075.

(26) Slowinski, K.; Fong, H. K. Y.; Majda, M. *J. Am. Chem. Soc.* **1999**, *121*, 7257.

(27) (a) York, R. L.; Nguyen, P. T.; Slowinski, K. *J. Am. Chem. Soc.* **2003**, *125*, 5948. (b) York, R. L.; Slowinski, K. *J. Electroanal. Chem.* **2003**, *550*, 327.

(28) Rampi, M. A.; Whitesides, G. M. *Chem. Phys.* **2002**, *281*, 373.

(29) Selzer, Y.; Salomon, A.; Cahen, J. *J. Am. Chem. Soc.* **2002**, *124*, 2886.

(30) Weiss, E. A.; Chiechi, R. C.; Kaufman, G. K.; Kriebel, J. K.; Li, Z.; Duati, M.; Rampi, M. A.; Whitesides, G. M. *J. Am. Chem. Soc.* **2007**, *129*, 4336.

(31) Chiechi, R. C.; Weiss, E. A.; Dickey, M. D.; Whitesides, G. M. *Angew. Chem., Int. Ed.* **2008**, *47*, 142.

**Electrical Characteristics of the Junctions with Top-Electrodes of Ga<sub>2</sub>O<sub>3</sub>/EGaIn.** Figure 1 shows an idealized schematic of the junctions. The outer layer of the EGaIn comprises oxides of gallium, of which Ga<sub>2</sub>O<sub>3</sub> is the most stable.<sup>32</sup> We believe that the gallium oxide film is responsible for the apparent non-Newtonian behavior of the Ga<sub>2</sub>O<sub>3</sub>/EGaIn, and for its ability to hold a conical shape at rest and yet flow upon application of shear stress.<sup>32</sup> The self-passivating layer of Ga<sub>2</sub>O<sub>3</sub> is only a few atomic layers thick when formed by oxidation of EGaIn in a controlled atmosphere of molecular oxygen;<sup>33</sup> we do not know how thick it is in the junctions we report here, especially after the repeated mechanical manipulation involved in making multiple contacts.<sup>34</sup> The nature of the contact between the Ga<sub>2</sub>O<sub>3</sub>/EGaIn and the SAM is unknown, although we suspect it is conformal on small scales (nm), but probably not conformal on large scales ( $\mu\text{m}$ ).<sup>35</sup> We assume that the contact of the Ga<sub>2</sub>O<sub>3</sub>/EGaIn top-electrodes with the top-surface of the SAMs is not covalent (we assume a van der Waals contact, although possibly with a hydrogen-bonding dative interaction involving the gallium and oxygen ions and the Fc group).

Lorenz et al. studied crystals of Ga<sub>2</sub>O<sub>3</sub> prepared by several methods: crystals grown from solutions of Ga<sub>2</sub>O<sub>3</sub> in Ga showed resistivity on the order of 1  $\Omega$  cm, while crystals grown from vapor under oxidizing conditions were significantly more resistive ( $>10^6$   $\Omega$  cm).<sup>36</sup> Thus, the resistivity of Ga<sub>2</sub>O<sub>3</sub> seems to correlate with the amount of oxygen present at growth. It is difficult to predict the resistivity of Ga<sub>2</sub>O<sub>3</sub> formed by spontaneous oxidation of the surface of Ga<sub>2</sub>O<sub>3</sub>/EGaIn at room temperature without knowing the crystallinity, phase, or concentration of defects of the material. The uncertainties in the thickness and continuity of the layer of Ga<sub>2</sub>O<sub>3</sub> complicate accurate estimation of the resistance of this layer; fortunately, for measures of rectification ratios, these uncertainties largely cancel.

We hypothesize that for a typical junction, the resistance of the layer of Ga<sub>2</sub>O<sub>3</sub> is several orders of magnitude less than the total resistance of the junction over the range of voltages applied and that the observed rectification of junctions of Ag<sup>TS</sup>-SC<sub>11</sub>Fc//Ga<sub>2</sub>O<sub>3</sub>/EGaIn originates from the chemical composition of the junctions, and not from the layer of Ga<sub>2</sub>O<sub>3</sub> or the SAM//Ga<sub>2</sub>O<sub>3</sub> interface. We have been able to carry out qualitative measurements; we outline these experiments later. Still, more experiments will be required to define completely the influence of the layer of Ga<sub>2</sub>O<sub>3</sub> on the  $J(V)$  characteristics of these junctions. Fortunately, measurement of rectification provides one way of minimizing the importance of this part of the junction.

**Protective Layers in Tunneling Junctions.** It seems that the four systems, each with its own generic problems, that generate usefully stable SAM-based tunneling junctions and make it possible to study charge transport across SAMs share one common element: they all incorporate a protective layer. (i) The polymer system reported by Akkerman et al. uses a layer of conducting polymer between the SAM and the Au top-electrode,

(ii) the Hg-drop with Hg or metal bottom-electrodes system uses a short chain-SAM between the Hg top-electrode and the SAM, (iii) the Hg-drop with Si bottom-electrodes system uses a layer of SiO<sub>2</sub> between the Si bottom-electrode and the SAM, and (iv) the system we report here uses a layer of Ga<sub>2</sub>O<sub>3</sub> between the EGaIn top-electrode and the SAM. These protective layers make it possible to generate SAM-based tunneling junctions, but also introduce ambiguities in the interpretation of data generated by these junctions caused by the protective layer.

**Rectification in Tunneling Junctions.** Four different mechanisms for molecular rectification have been discussed: (i) tunneling in donor- $\sigma$ -acceptor type of molecules,<sup>37</sup> (ii) formation of a Schottky barrier due to a difference in the work functions of the electrodes,<sup>38</sup> (iii) asymmetric placement of an electron donor or acceptor between two electrodes,<sup>39,40</sup> and (iv) resonant tunneling via a single molecular orbital.<sup>41,42</sup> Although rectification (usually with values of  $R$  in the range of 1–10) has been claimed in a variety of junctions,<sup>43</sup> the reliability of these measurements is untested statistically, and details of the mechanism(s), if indeed the rectification is real, remain elusive. Typically, few details have been made available on the stability of devices, or on the reproducibility of rectification from sample to sample; thus, statistical analysis of the data is largely absent from the literature on molecular rectification, and the statistical difference of these values from  $R = 1$  (e.g., no rectification) has never been established. Ashwell et al.<sup>11</sup> reported tunneling junctions that incorporated SAMs, or bilayers, of molecules with complex chemical structures (SAMs of bis-[*N*-(10-decyl)-5-(4-dimethylaminobenzylidene)-5,6,7,8-tetrahydroisoquinolinium]-disulfide diiodide and metathesis with the tetrasodium salt of copper(II) phthalocyanine-3,4',4'',4'''-tetrasulfonate) in STM-based tunneling junctions. These studies reported rectification ratios  $R$  up to 3000, but gave little information about the mechanism of rectification, the structures of the SAMs, or the stability and reproducibility of these systems.

Gorman et al. and Walker et al. did not observe rectification for SAMs of SC<sub>11</sub>Fc using conductive probe AFM (cpAFM) or STM at  $\pm 1.5$  V, but did report negative differential resistance (NDR).<sup>44</sup> The mechanism they proposed involved off- and on-resonant tunneling and oxidation and reduction of the Fc moiety; this proposal had little experimental support. Lindsay et al. showed that the NDR effect of these SAMs is not a molecular property because the NDR was: (i) irreversible, (ii) almost completely absent when oxygen levels were reduced, (iii) never observed in the retrace of a scan, and (iv) only present in 5% of the cases in both the negative and the positive directions of

- (32) Dickey, M. D.; Chiechi, R. C.; Larson, R. J.; Weiss, E. A.; Weitz, D. A.; Whitesides, G. M. *Adv. Funct. Mater.* **2008**, *18*, 1097.  
 (33) Tostmann, H.; DiMasi, E.; Ocko, B. M.; Deutsch, M.; Pershan, P. S. *J. Non-Cryst. Solids* **1999**, *250–252*, 182.  
 (34) Differences in thickness of the GaO<sub>x</sub> may be partially responsible for the variance of 2 orders in magnitude in the observed current densities from junction to junction.  
 (35) Preliminary scanning electron micrographs show that the conically shaped tips of Ga<sub>2</sub>O<sub>3</sub>/EGaIn are rough. We are now performing experiments to quantify the surface roughness of the conically shaped tips of Ga<sub>2</sub>O<sub>3</sub>/EGaIn.  
 (36) Lorenz, M. R.; Woods, J. F.; Gambino, R. J. *J. Phys. Chem. Solids* **1967**, *28*, 403.

- (37) Aviram, A.; Ratner, M. A. *Chem. Phys. Lett.* **1974**, *29*, 277.  
 (38) Metzger, R. M. *Chem. Rev.* **2003**, *103*, 3803.  
 (39) Liu, R.; Ke, S.-H.; Yang, W.; Baranger, H. U. *J. Chem. Phys.* **2006**, *124*, 024718.  
 (40) Kornilovitch, P. E.; Bratkovsky, A. M.; Williams, R. S. *Phys. Rev. B* **2002**, *66*, 165436.  
 (41) Peterson, I. R.; Vuillaume, D.; Metzger, R. M. *J. Phys. Chem. A* **2001**, *105*, 4702.  
 (42) Shumate, W. J.; Mattern, D. L.; Jaiswal, A.; Dixon, D. A.; White, T. R.; Burgess, J.; Honciu, A.; Metzger, R. M. *J. Phys. Chem. B* **2006**, *110*, 11146.  
 (43) (a) Kitagawa, K.; Morita, T.; Kimura, S. *J. Phys. Chem. B* **2005**, *109*, 13906. (b) Ashwell, G. J.; Ewinton, J.; Robinson, B. J. *Chem. Commun.* **2006**, 618. (c) Honciu, A.; Jaiswal, A.; Gong, A.; Ashworth, K. W.; Spangler, C.; Peterson, I. R.; Dalton, L. R.; Metzger, R. M. *J. Phys. Chem. B* **2005**, *109*, 857.  
 (44) (a) Tivanski, A.; Walker, G. C. *J. Am. Chem. Soc.* **2005**, *127*, 7647. (b) Gorman, C. B.; Carroll, R. L.; Fuierer, R. R. *Langmuir* **2001**, *17*, 6923. (c) Wassel, R. A.; Credo, G. M.; Fuierer, R. R.; Feldheim, D. L.; Gorman, C. B. *J. Am. Chem. Soc.* **2004**, *127*, 7647.

the scan.<sup>45</sup> They proposed that reaction of the charged species with oxygen caused the anomalies in the  $I(V)$  curves.

In a careful study that is important for the work we report in this Article, Zandvliet et al. reported a STM study (using a tungsten STM-tip) of  $SC_nFc$  (with  $n = 3, 5, \text{ or } 11$ ) embedded in a SAMs of  $SC_{n-1}CH_3$  ( $n = 8 \text{ or } 12$ ) on Au.<sup>46</sup> Measurements of  $I(V)$  curves measured on the  $SC_{11}Fc$  molecules embedded in the matrix of the alkanethiolates rectified currents with rectification ratios of 5–10, while  $I(V)$  curves measured on the alkanethiolates were (nearly) symmetric. The authors did not propose a mechanism for the observed rectification. This result is important for the results reported in the current Article because the same molecules,  $SC_{11}Fc$ , rectify currents in a junction entirely different from the one we describe. This result is one of three that strongly suggests that observation of rectification in  $Ga_2O_3/EGaIn$  based-system is not an artifact of, for example, redox behavior of the  $Ga_2O_3$  film, or formation of filaments bridging the SAM. Although these two types of tunneling junctions, STM-based tunneling junctions ( $R \approx 5\text{--}10$ ) and a tunneling junction of  $Ag^{TS}\text{-}SC_{11}Fc//Ga_2O_3/EGaIn$  ( $R \approx 30\text{--}300$ ), give different values of  $R$ , they also have different environments for the Fc groups and different densities of Fc groups.

**Statistical Analysis.** In junctions investigated by scanning probes,<sup>47</sup> as well as in break junctions,<sup>48</sup> statistical analysis of large sets of data is common<sup>2</sup> and, indeed, necessary to account for, for example, the difference in conformation and connectivity, and variations in the number of molecules inside the junctions. By contrast, statistical analysis on SAM-based tunneling junctions is essentially absent in the literature. Many studies report or imply a low yield (<5% and much lower<sup>1,14</sup>) of working devices, but do not clearly define what constitutes a “working device”, or provide explicit criteria for selecting “representative data”. For instance, Vuillaume et al.<sup>9</sup> reported a “statistical analysis” on the rectification ratio of a small number of junctions (20–30) with donor–bridge–acceptor type of molecules covalently linked to Si/SiO<sub>2</sub> bottom-electrodes with vapor-deposited Al (possibly with aluminum oxide) top-electrodes. The authors did not discriminate artifact from real data and did not define “representative data”. We consider their major result, one device that rectified currents with a rectification ratio of 37 out of a set of 29 devices, to be an artifact, because 27 of 29 devices showed rectification ratios in the range of 2–12 with the mean value of  $R$  of  $\sim 5$ .

Kim et al. recently performed a careful statistical analysis on 13 440 devices and reported a 1.2% yield of working junctions incorporating evaporated top contacts.<sup>1</sup> This yield was obtained by skilled and experienced users; most procedures reported in the literature probably had much lower yields, and discrimination between “data” and “artifacts” was not straightforward. Kim et al. analyzed their data by fitting Gaussians to histograms of the current densities. Only data within  $3\sigma_{\log}$  (where  $\sigma_{\log}$  is the log-standard deviation, see below) were considered as “representative” data for their junctions and selected for further analysis, for instance, to determine the decay coefficient  $\beta$ .<sup>1</sup> Because of the clear and thoughtful use of criteria for

selecting representative data, Kim et al. were able to draw meaningful conclusions, even from a low yield of working devices.

**Metal–Oxide in SAM-Based Tunneling Junctions.** A layer of metal–oxide, or other semiconductors, in SAM-based tunneling junctions may complicate the interpretation of the data generated by those junctions or may dominate their characteristics. Tunneling junctions that contain semiconductors may form Schottky barriers.<sup>16,17,38,49</sup> These junctions can rectify currents, and their characteristics may be independent of the chemical structure of the molecules in these junctions. Junctions with a redox-active layer of metal oxide can rectify currents. McCreery et al. have shown spectroscopically that junctions of the type carbon-organic layer/TiO<sub>2</sub>/Au rectify currents induced by redox reactions in these junctions.<sup>50</sup> In junctions with an organic layer of nitroazobenzene, both the organic layer and the layer of TiO<sub>2</sub> are redox-active, and the redox reactions may be driven by the large electric fields across these nanoscale junctions (1.0 V over 1 nm corresponds to an electric field of 1.0 GV/m).<sup>51</sup> These junctions rectified currents and the mechanism of charge transport involved redox reactions of both the layer of nitroazobenzene and TiO<sub>2</sub>. Junctions without the redox-active organic layer, or without the layer of TiO<sub>2</sub>, did not rectify currents.

The junctions reported in this Article have a layer of  $Ga_2O_3$  between the SAM and the EGaIn top-electrode. We discuss the influence of this layer of  $Ga_2O_3$  on the  $J(V)$  characteristics of the junctions below.

**Wet Electrochemistry of Fc-Terminated SAMs.** This Article describes rectifying tunneling junctions with SAMs of  $SC_{11}Fc$ . These SAMs have been extensively characterized electrochemically and structurally.<sup>52</sup> Ideal electrochemical behavior (i.e., symmetrical cyclic voltammograms) has been observed for Fc-terminated alkanethiolate SAMs in contact with electrolyte, when the surface density of the Fc units ( $\Gamma_{Fc}$ ) was low, and when the SRFc species were diluted (by a factor of 10 or more) by alkanethiolates that were not electrochemically active.<sup>53</sup> Densely packed SAMs (i.e., large values of  $\Gamma_{Fc}$ ) show abnormal peak broadening, peak splitting, and the appearance of a new wave at higher potentials.<sup>53</sup> A number of explanations may account for (or contribute to) this observation: steric crowding of the Fc moieties, double-layer effects, differences arising from the polycrystalline Au surface, and differential order within the SAM.<sup>54</sup> The most widely accepted explanation is that the peak observed at lower potentials arises from Fc moieties that do not interact strongly with their neighbors, while the wave at higher potentials arises from Fc moieties in close proximity to other Fc moieties.<sup>55</sup> Electrochemical characterization of SAMs of  $SC_{11}Fc$  gives valuable information of the quality, structure, and surface coverage of these SAMs.

## Experimental Details

The Supporting Information gives the experimental details of the formation of ultraflat Ag surfaces, SAMs, and the junctions.

(45) He, J.; Lindsay, S. M. *J. Am. Chem. Soc.* **2005**, *127*, 11932.

(46) Müller-Meskamp, L.; Karthäuser, S.; Zandvliet, H. J. W.; Homberger, M.; Simon, U.; Waser, R. *Small* **2009**, *5*, 496.

(47) Li, X. L.; He, J.; Hihath, J.; Xu, B. Q.; Lindsay, S. M.; Tao, N. J. *J. Am. Chem. Soc.* **2006**, *128*, 2135.

(48) (a) Muller, C. J.; Van Ruitenbeek, J. M.; De Jongh, L. J. *Phys. Rev. Lett.* **1992**, *69*, 140. (b) Reed, M. A.; Zhou, C.; Muller, C. J.; Burgin, T. P.; Tour, J. M. *Science* **1997**, *278*, 252.

(49) Cahen, D.; Hodes, G. *Adv. Mater.* **2002**, *14*, 789.

(50) McCreery, R. L.; Kalakodimi, R. P. *Phys. Chem. Chem. Phys.* **2006**, *8*, 2572.

(51) Wu, J.; McCreery, R. L. *J. Electrochem. Soc.* **2009**, *156*, 29.

(52) Chidsey, C. E. D. *Science* **1991**, *251*, 919.

(53) Chidsey, C. E. D.; Bertozzi, C. R.; Putvinski, T. M.; Muijsce, A. M. *J. Am. Chem. Soc.* **1991**, *112*, 4301.

(54) Rowe, G. K.; Creager, S. E. *Langmuir* **1994**, *10*, 1186.

(55) (a) Lee, L. Y. S.; Sutherland, T. C.; Rucareanu, S.; Lennox, R. B. *Langmuir* **2006**, *22*, 4438. (b) Valincius, G.; Niaura, G.; Kazakevičienė, B.; Talaikyte, Z.; Kazemekaite, M.; Butkus, E.; Razumas, V. *Langmuir* **2004**, *20*, 6631.

We performed statistical analyses to characterize the distribution of  $R$  and the yield of working devices (see below, and in the Supporting Information for more details). In all experiments, we grounded the  $\text{Ag}^{\text{TS}}$  bottom-electrode and biased the  $\text{Ga}_2\text{O}_3/\text{EGaIn}$  top-electrode, and we used the same electrical circuit to measure  $J(V)$  curves as reported earlier.<sup>30</sup> A camera (Edmund Industrial Optics) captured a magnified image of the junction from the side, and we measured the diameter of the junction on the computer screen. The contact areas of the  $\text{Ga}_2\text{O}_3/\text{EGaIn}$  top-electrodes with the SAMs ranged from  $\sim 100$  to  $\sim 300 \mu\text{m}^2$ .

### Experimental Design

We used Ag surfaces rather than Au surface because the tilt angle of SAMs of alkanethiolates on Ag ( $\sim 11^\circ$ ) is much smaller than on Au ( $\sim 30^\circ$ ).<sup>3</sup> SAMs with larger tilt angles form larger defect sites at phase-domain boundaries than do those with smaller tilt angles. Template-stripped Ag surfaces have much lower surface roughness and larger grain sizes than as-deposited (AS-DEP, substrates deposited by electron-beam evaporation) Ag surfaces.<sup>30</sup> These characteristics of the  $\text{Ag}^{\text{TS}}$  surface result in a density of defects in SAMs of alkanethiolates lower than those of SAMs formed on the top surfaces of Ag AS-DEP.

The Fc moiety has a highest occupied molecular orbital (HOMO) that is close in energy to the Fermi levels of the metal electrodes. In addition, the Fc moiety is a relatively stable, redox-active moiety.<sup>56</sup> The length of the alkyl chain connecting the Fc moiety to the  $\text{Ag}^{\text{TS}}$  surface is important. Long alkyl chains ( $C_n > 15$ ) can fold over and allow the Fc moiety to reach back toward the surface (so-called “back-bending”<sup>57</sup>), and short alkyl chains ( $C_n < 8$ ) may allow metal filaments to form between electrodes and to cause shorts in the junctions. The properties of SAMs of  $\text{SC}_{11}\text{Fc}$  alkanethiolates on  $\text{Ag}^{\text{TS}}$  give SAM-based tunneling junctions that are stable over the times required for measurement of tunneling currents and that have structures that are reasonably well understood.

The junctions with  $\text{Ga}_2\text{O}_3/\text{EGaIn}$  as a top contact are stable, easy to assemble, and reproducible (especially junctions incorporating  $\text{SC}_{11}\text{Fc}$ ; junctions of alkanethiolates are satisfactorily reproducible, but require the hands of a skilled operator).<sup>31</sup> These characteristics allow the study of charge transport as a function of the structure of the SAM through the collection of statistically large numbers of data. The junctions have three characteristics that are ill-defined: (i) the morphology of the thin layer of  $\text{Ga}_2\text{O}_3$  on the surface of EGaIn; we do not know the exact thickness and the surface roughness of the layer of  $\text{Ga}_2\text{O}_3$  in the junctions; X-ray studies showed that the self-limiting layer of  $\text{Ga}_2\text{O}_3$  is 0.5–1.0 nm thick when formed on the surface of a stable film of liquid alloy,<sup>33</sup> but is probably thicker in our junctions due to mechanical deformation, fracture, and reformation when we form the cone-shaped top-electrodes;<sup>35</sup> (ii) the unknown resistivity of the layer of  $\text{Ga}_2\text{O}_3$ ; “gallium oxide” is a semiconductor whose resistivity depends on the conditions of formation<sup>36</sup> but is probably several orders of magnitude less than that of the most resistive element (the SAM) in the junction (see below); and (iii) the interface between the SAM and the layer of  $\text{Ga}_2\text{O}_3$ ; the exact nature of this interface is not known, and our estimate of the area of contact in the junction is based on the assumption of conformal contact. We assume that the  $\text{Ga}_2\text{O}_3$  forms a van der Waals contact with both Fc- and  $\text{CH}_3$ -terminated SAMs.

The distribution of values of  $J$  at a particular value of  $V$  that we collected suggests that values of  $\log(J)$  in tunneling junctions are normally distributed. Other research groups have also observed this so-called “log-normal” distribution for current densities.<sup>1</sup> We have, accordingly, analyzed the distributions of the values of  $J$  on the log scale to determine the reproducibility of the data from these junctions, the rectification ratios, and the yields of working

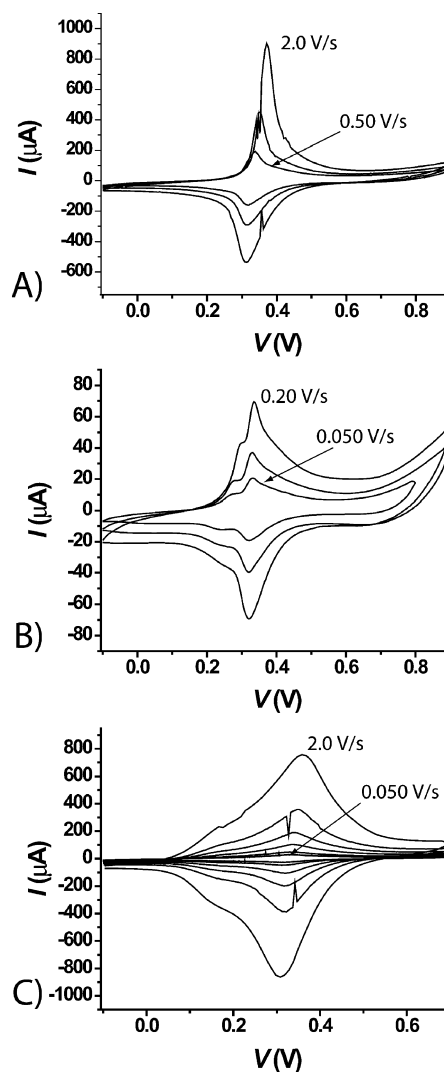


**Figure 2.** Cyclic voltammograms of SAMs of  $\text{SC}_{11}\text{Fc}$  on Au. The SAMs were formed for 24 h (A and B) or 10 min (C) using a 1 mM ethanolic solution of  $\text{HSC}_{11}\text{Fc}$  at room temperature under an argon atmosphere (aqueous 1 M  $\text{HClO}_4$  as electrolyte solution, and potentials vs  $\text{Ag}/\text{AgCl}$ ): (A) scan rate = 2.0, 1.0, and 0.50 V/s; (B) scan rate = 0.200, 0.100, and 0.050 V/s; (C) scan rate = 2.0, 1.0, 0.50, 0.200, 0.100, and 0.050 V/s.

junctions. Our justification for a log-normal treatment in our analysis is that in junctions where tunneling is the dominant mechanism of charge-transport,  $J$  depends exponentially on the distance between the top- and bottom-electrodes  $d$  ( $J \propto \exp(-\beta d)$ ). Although  $J$  is ideally determined by the thickness of the SAM, in reality defects in the SAM and the electrodes cause variations in the effective  $d$ , variations that are, presumably, normally distributed. We therefore believe that the log-normal distribution of  $J$  is the result of the normal distribution of the effective distance between the top- and bottom-electrodes. The rectification ratio is the quotient of two log-normally distributed parameters,  $|J(V)|$  and  $|J(-V)|$ , and is for this reason also log-normally distributed.

### Results and Discussion

**$\text{SC}_{11}\text{Fc}$  SAMs on  $\text{Au}^{\text{TS}}$  Electrodes Are Densely Packed.** We used cyclic voltammetry to determine the surface coverage, the structure, and the energy of the highest occupied molecular orbital (HOMO). Figure 2 shows cyclic voltammograms of SAMs of  $\text{SC}_{11}\text{Fc}$  on  $\text{Au}^{\text{TS}}$  electrodes (aqueous 1 M  $\text{HClO}_4$  electrolyte) with a Pt counter-electrode and a  $\text{Ag}/\text{AgCl}$  reference electrode. Integration of the cyclic voltammogram gives the total

(56) Weber, K.; Hockett, L.; Creager, S. *J. Phys. Chem. B* **1997**, *101*, 8286.  
(57) Auletta, T.; van Veggel, F. C. J. M.; Reinhoudt, D. N. *Langmuir* **2002**, *18*, 1288.

**Table 1.** Statistics of the Ag<sup>TS</sup>-SAM//Ga<sub>2</sub>O<sub>3</sub>/EGaIn Junctions

type of SAM	total substrates <sup>a</sup>	total junctions <sup>b</sup>	total traces in histogram	short-circuited junctions (%)	unstable junctions (%)	yield (%) <sup>c</sup>
SC <sub>11</sub> Fc	10	53	997	3 (5.6)	4 (7.4)	87
SC <sub>10</sub> CH <sub>3</sub>	4	23	415	4 (17)	3 (13)	70
SC <sub>14</sub> CH <sub>3</sub>	5	14	287	0 (0)	3 (21)	79

<sup>a</sup> We used 10 different template-stripped substrates from at least two wafers coated with 500 nm of Ag. <sup>b</sup> We formed the SAMs at the template-stripped Ag electrodes and contacted the SAMs with conically shaped electrodes of Ga<sub>2</sub>O<sub>3</sub>/EGaIn to complete the junctions. <sup>c</sup> We define a junction as “working” when its *J(V)* characteristics fall within three log-standard deviations from the mean value of *J*.

charge ( $Q_{\text{tot}}$ ), from which the surface coverage of the Fc units ( $\Gamma_{\text{Fc}} = \text{mol}/\text{cm}^2$ ) can be calculated directly using eq 2, where *n* is the number of electrons per mole of reaction, *F* is the Faraday constant, and *A* is the surface area of the electrode exposed to the electrolyte solution (0.44 cm<sup>2</sup>):<sup>58</sup>

$$\Gamma_{\text{Fc}} = Q_{\text{tot}}/nFA \quad (2)$$

We measured a  $Q_{\text{tot}}$  of  $(2.1 \times 10^{-5}) \pm (0.2 \times 10^{-5})$  C; this value implies  $\Gamma_{\text{Fc}} = (4.9 \pm 0.4) \times 10^{-10}$  mol/cm<sup>2</sup>. This density of Fc groups is close to the theoretical value  $\Gamma_{\text{Fc}} = 4.5 \times 10^{-10}$  mol/cm<sup>2</sup> calculated assuming a hexagonal packing, with Fc treated as a sphere with a diameter of 6.6 Å.<sup>60</sup> Thus, the SAMs of SC<sub>11</sub>Fc are densely packed, but the alkyl chains probably have a lower degree of order than that of alkanethiolates due to steric interactions between the relative bulky Fc moieties.<sup>59</sup> The diameter of a Fc moiety is about 6.6 Å,<sup>60</sup> while the diameter of the alkyl chains is 4.5 Å.<sup>3</sup>

We estimated the energy level for the HOMO ( $E_{\text{HOMO}}$ ) to be  $\sim -5.0$  eV, relative to vacuum, from the cyclic voltammogram, using eq 3, where  $E_{\text{abs,NHE}}$  is the absolute potential energy of the normal hydrogen electrode (−4.5 eV), and  $E_{1/2,\text{NHE}}$  is the formal half-wave potential versus normal hydrogen electrode (which is 0.466 eV):

$$E_{\text{HOMO}} = E_{\text{abs,NHE}} - eE_{1/2,\text{NHE}} \quad (3)$$

We observed a single oxidation wave in the cyclic voltammograms of SAMs of SC<sub>11</sub>Fc on Au<sup>TS</sup> when we incubated the Au in the thiol-containing solutions for long times (18–24 h; Figure 2A). For SAMs formed over only 10 min, two oxidation waves appeared in the cyclic voltammograms (Figure 2C). At low scan rates, we always observed two waves (Figure 2B). The most widely accepted explanation for the wave-splitting is that the wave at lower potentials originates from Fc moieties that do not interact strongly with their neighbors, while the wave at higher potentials arises from strongly interacting Fc moieties. The wave at higher oxidation potentials is dominant. This observation indicates that the SAMs are densely packed and have a low number of defects. The facts that there is a small difference between the peak cathodic and peak anodic potentials ( $E_{\text{pc}}$  and  $E_{\text{pa}}$ , respectively), and that this difference increases with increasing scan rate, suggest slow electron transfer processes due to the presence of the long alkyl chains and order in the SAM.<sup>56</sup>

**Measurements of Current Density in SAM-Based Tunneling Junctions.** Table 1 shows the number of junctions that we measured, the number of *J(V)* curves that we collected, and

the yields of the Ag<sup>TS</sup>-SC<sub>11</sub>Fc//Ga<sub>2</sub>O<sub>3</sub>/EGaIn, Ag<sup>TS</sup>-SC<sub>10</sub>CH<sub>3</sub>//Ga<sub>2</sub>O<sub>3</sub>/EGaIn, and Ag<sup>TS</sup>-SC<sub>14</sub>CH<sub>3</sub>//Ga<sub>2</sub>O<sub>3</sub>/EGaIn junctions (see the Supporting Information for details).

Our objective was to establish the reproducibility of *R* and to determine the yield and stability of working devices. To do so, we analyzed *R* for 53 Ag<sup>TS</sup>-SC<sub>11</sub>Fc//Ga<sub>2</sub>O<sub>3</sub>/EGaIn junctions. In total, we recorded 997 *J(V)* traces (1 trace = 0 V → +1 V → −1 V → 0 V) on these 53 junctions assembled on 10 different Ag<sup>TS</sup> substrates (five to six junctions per substrate), starting with three different Ag-coated wafers. For each junction, we carried out 21 *J(V)* traces, after which we stopped the experiment and disassembled the junction, so that all junctions would have equal weight in the statistical analysis. Except for three junctions that short-circuited on the first *J(V)* trace, and four junctions that were unstable (due either to a short-circuit or to large fluctuations in current density) in subsequent *J(V)* traces, all remaining junctions continued to rectify for the complete set of 21 *J(V)* traces. Current density often gradually decreased (by a factor of 2–5) during these measurements; because measurements of rectification compare currents flowing through the same junction in opposite directions, this gradual decrease in current density does not complicate the rectification ratio.

To demonstrate the stability of the rectifying junctions, we measured 100 traces on each of five junctions (see below): we also measured 200 traces on one junction. (None of these junctions were included in the statistical analysis described above.) One junction short-circuited after 90 traces, but the remaining five continued to rectify until the measurement was terminated: these junctions are, thus, substantially more stable than most junctions based on SAMs.

For all types of junctions, we observed log-normal distributions in both *J* (at a particular voltage) and *R*; as such, all values of *J* and *R* reported in this work represent the log-mean ( $\mu_{\log}$ ) of a distribution, accompanied by the log-standard deviation ( $\sigma_{\log}$ ) in parentheses.<sup>61</sup> A similar analysis of Ag<sup>TS</sup>-SC<sub>10</sub>CH<sub>3</sub>//Ga<sub>2</sub>O<sub>3</sub>/EGaIn and Ag<sup>TS</sup>-SC<sub>14</sub>CH<sub>3</sub>//Ga<sub>2</sub>O<sub>3</sub>/EGaIn junctions showed only very slight rectification (*R* = 1.5 (1.4) and 2.1 (2.5), respectively) with higher currents at positive voltages than at negative voltages, as opposed to higher currents at negative voltages than at positive voltages observed in Ag<sup>TS</sup>-SC<sub>11</sub>Fc//Ga<sub>2</sub>O<sub>3</sub>/EGaIn junctions. In total, 23 Ag<sup>TS</sup>-SC<sub>10</sub>CH<sub>3</sub>//Ga<sub>2</sub>O<sub>3</sub>/EGaIn junctions were assembled at five different Ag<sup>TS</sup> substrates on glass obtained from two different Ag-coated wafers. Of these 23 junctions, four immediately shorted, and three were not stable and shorted after 3–10 traces. In total, we recorded 415 traces that were used in the analysis.

For the Ag<sup>TS</sup>-SC<sub>10</sub>CH<sub>3</sub>//Ga<sub>2</sub>O<sub>3</sub>/EGaIn junctions, we found that, at  $\pm 1$  V, *R* = 1.5 (1.4), from data collected across a total of 23 junctions assembled on four Ag<sup>TS</sup> substrates.<sup>62</sup> Thus, 68% of the distribution of *R* was within the range of 1.1–2.1.

(61) A log-normally distributed variable is one whose logarithm is normally distributed. For instance, *R* is log-normally distributed when log(*R*) is normally distributed. If *m* and *s* are the mean and standard deviation of log(*R*), then the log-mean ( $\mu_{\log}$ ) and log-standard deviation ( $\sigma_{\log}$ ) of *R* are given by  $10^m$  and  $10^s$ , respectively. Because 68% of the distribution of log(*R*) lies between *m*−*s* and *m*+*s*, 68% of the distribution of *R* lies between  $10^{m-s}$  and  $10^{m+s}$  or, equivalently, between  $\mu_{\log}/\sigma_{\log}$  and  $\mu_{\log} \times \sigma_{\log}$ . When not explicitly stated, we report the statistics of log-normal distributions according to the format *R* =  $\mu_{\log}(\sigma_{\log})$ .

(62) To report all rectification ratios consistently as values greater than or equal to unity, and because junctions incorporating alkanethiolates show enhanced current at positive bias, we use the definition of *R* for such junctions so that  $R = |J(V)|/|J(-V)|$  for junctions in which  $|J(V)| > |J(-V)|$ .

(58) Bard, A. J.; Faulkner, L. R. *Electrochemical Methods: Fundamentals and Applications*; John Wiley & Sons: New York, 2001.

(59) Han, S. W.; Seo, H.; Chung, Y. K.; Kim, K. *Langmuir* **2000**, *16*, 9493.

(60) Rowe, G. K.; Creager, S. E. *Langmuir* **1991**, *7*, 2307.

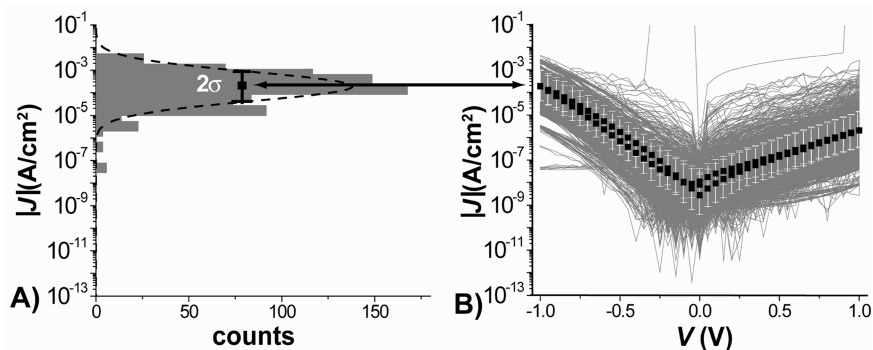


**Figure 3.** (A) Histogram of all of the values (997 in total) of  $|J|$  for  $V = -1.0$  V measured across  $\text{Ag}^{\text{TS}}\text{-SC}_{11}\text{Fc//Ga}_2\text{O}_3\text{/EGaIn}$  junctions with a Gaussian fit to this histogram. The peak of the Gaussian in (A) gives the log-mean value of  $J$ , shown at  $V = -1.0$  V as one point on the average trace (B, black), while the log-standard deviation of the Gaussian in (A) provides the error bars for the same point. The log-standard deviation is indicated in the histogram. Similarly, fitting a separate Gaussian for each voltage yields the remainder of the values and error bars shown in the average trace. (B) Average trace (black) of  $\text{Ag}^{\text{TS}}\text{-SC}_{11}\text{Fc//Ga}_2\text{O}_3\text{/EGaIn}$  junctions superimposed over all 997 traces (gray) collected on these junctions. The three traces from junctions that short-circuited lie outside the scale of the figure ( $|J| \approx 10^4$  A/cm<sup>2</sup>) and are not shown. The error bars (white) indicate the log-standard deviation.

For junctions of the form  $\text{Ag}^{\text{TS}}\text{-SC}_{14}\text{CH}_3\text{/Ga}_2\text{O}_3\text{/EGaIn}$ , 14 junctions were assembled at five  $\text{Ag}^{\text{TS}}$ -substrates on glass. These  $\text{Ag}^{\text{TS}}$  substrates were obtained from two different Ag-coated wafers. The rectification ratio for these junctions was  $R = 2.1$  (2.5), and the range  $8.4 \times 10^{-1}$  to  $5.3$  encompassed 68% of this major peak. These experiments demonstrate that the large rectification observed in tunneling junctions incorporating  $\text{SC}_{11}\text{Fc}$  requires the ferrocene moiety and is not a general property of  $\text{Ag}^{\text{TS}}\text{-SR//Ga}_2\text{O}_3\text{/EGaIn}$  junctions (see below for more details).

**Statistical Analysis of the Current Densities.** Figure 3 shows the procedure for the statistical analysis of the  $\text{Ag}^{\text{TS}}\text{-SC}_{11}\text{Fc//Ga}_2\text{O}_3\text{/EGaIn}$  junctions. Figure 3A shows the histogram of all 997 values of  $|J|$  collected at  $V = -1.0$  V. A nonlinear least-squares fitting algorithm fitted a Gaussian to the entire log-normally distributed histogram and gave the log-mean and log-standard deviation for  $|J|(-1$  V). We stress that the fitting algorithm considered all 997 values of  $|J|$  in the histogram, with no exceptions, when fitting the Gaussian.

Plotting and fitting the histogram of  $J$  for each voltage in a  $J(V)$  trace yields the log-mean and log-standard deviation at each measured potential and allows the construction of the average trace (Figure 3B, black) containing each log-mean bounded with error bars defined by the corresponding log-standard deviation.<sup>63</sup> Figure 3B shows the average trace superimposed on all 997 traces (gray) recorded (we did not select data) on the  $\text{Ag}^{\text{TS}}\text{-SC}_{11}\text{Fc//Ga}_2\text{O}_3\text{/EGaIn}$  junctions. The same procedure yielded the average traces for the junctions incorporating alkanethiolates. Figure 4 shows the average traces of  $|J|$  as a function of the applied voltage ( $V$ ) for all junctions. We observed that the current densities for the  $\text{Ag}^{\text{TS}}\text{-SC}_{10}\text{CH}_3\text{/Ga}_2\text{O}_3\text{/EGaIn}$  and  $\text{Ag}^{\text{TS}}\text{-SC}_{14}\text{CH}_3\text{/Ga}_2\text{O}_3\text{/EGaIn}$  junctions are similar (within 1 order of magnitude) to those obtained with a top-electrode of  $\text{Hg-SC}_{11}$ .<sup>64</sup>

**Statistical Analysis of the Rectification Ratios.** To analyze rectification in these junctions, we constructed and fitted

histograms for  $R$  rather than for  $J$ . Figure 5A shows a histogram of all 997 rectification ratios  $R$  (eq 1) calculated individually for each trace measured in the  $\text{Ag}^{\text{TS}}\text{-SC}_{11}\text{Fc//Ga}_2\text{O}_3\text{/EGaIn}$  junctions. The histogram contains all 997 values of  $R$  sorted into 100 logarithmically spaced bins over the interval  $(10^{-2}, 10^4)$ . The solid black line shows a nonlinear least-squares, Gaussian fit to the histogram of  $R$ ; the Gaussian fit gave  $R = 1.0 \times 10^2$  (3.0) (i.e.,  $\mu_{\log} = 1.0 \times 10^2$  and  $\sigma_{\log} = 3.0$ ). Thus, 68% of the distribution of  $R$  is within the range  $3.3 \times 10$  to  $3.0 \times 10^2$  ( $1.0 \times 10^2/3.0$  and  $1.0 \times 10^2 \times 3.0$ , respectively).

The  $\text{Ag}^{\text{TS}}\text{-SC}_{10}\text{CH}_3\text{/Ga}_2\text{O}_3\text{/EGaIn}$  (Figure 5B) and the  $\text{Ag}^{\text{TS}}\text{-SC}_{14}\text{CH}_3\text{/Ga}_2\text{O}_3\text{/EGaIn}$  junctions (Figure 5C) show a small current enhancement at the positive voltages, while  $\text{Ag}^{\text{TS}}\text{-SC}_{11}\text{Fc//Ga}_2\text{O}_3\text{/EGaIn}$  junctions show current enhancement at negative bias. As explained above, we define  $R$  for the  $\text{Ag}^{\text{TS}}\text{-SC}_{10}\text{CH}_3\text{/Ga}_2\text{O}_3\text{/EGaIn}$  and  $\text{Ag}^{\text{TS}}\text{-SC}_{14}\text{CH}_3\text{/Ga}_2\text{O}_3\text{/EGaIn}$  junctions as  $|J(+1$  V)/ $|J(-1$  V). Figure 5B shows the histogram of  $R$  for all  $\text{Ag}^{\text{TS}}\text{-SC}_{10}\text{CH}_3\text{/Ga}_2\text{O}_3\text{/EGaIn}$  junctions with  $R$  values sorted into 100 logarithmically spaced bins over the same interval as above. The black line represents a Gaussian fit, which gave a log-mean of  $R = 1.5$  (1.4). Thus, 68% of the distribution of the values of  $R$  is in the range of  $1.1$ – $2.1$ . Figure 5C shows the corresponding histogram of  $R$  for  $\text{Ag}^{\text{TS}}\text{-SC}_{14}\text{CH}_3\text{/Ga}_2\text{O}_3\text{/EGaIn}$  junctions. The Gaussian fit of the major peak yields  $R = 2.0$  (2.5) (68% of the data constituting the major peak lie between  $8.4 \times 10^{-1}$  and  $5.3$ ).

To determine whether the values of  $R$  for junctions of  $\text{Ag}^{\text{TS}}\text{-SC}_{10}\text{CH}_3\text{/Ga}_2\text{O}_3\text{/EGaIn}$  and  $\text{Ag}^{\text{TS}}\text{-SC}_{14}\text{CH}_3\text{/Ga}_2\text{O}_3\text{/EGaIn}$  differ significantly from unity (i.e., demonstrate rectification), we applied one-sample  $t$ -tests to the respective populations. For both populations, we calculated  $p$ , the probability that the null hypothesis, that  $R$  is unity, is true and found that  $p < 0.01\%$ . This value implies that the rectification observed in both types of junctions is statistically significant from unity.

Further, we used a two-sample  $t$ -test (see the Supporting Information for details) to determine whether the values of  $R$  for junctions of  $\text{Ag}^{\text{TS}}\text{-SC}_{10}\text{CH}_3\text{/Ga}_2\text{O}_3\text{/EGaIn}$  and  $\text{Ag}^{\text{TS}}\text{-SC}_{14}\text{CH}_3\text{/Ga}_2\text{O}_3\text{/EGaIn}$  differ significantly from each other. In this case, the null hypothesis has probability  $p$  of being true and states that these two junctions rectify current indistinguishably from one another. Again, we calculated that  $p < 0.01\%$ . This value indicates that not only are both values of  $R$  statistically greater than unity, they also differ significantly (in a statistical sense) from each other. Applying the above tests to the population of

(63) If  $\mu_{\log}$  is the log-mean and  $\sigma_{\log}$  is the log-standard deviation of  $J$  at a particular voltage, then for the corresponding point on the average trace the lower error bar lies at a value of  $\mu_{\log}/\sigma_{\log}$ , while the upper error bar lies at a value of  $\mu_{\log} \times \sigma_{\log}$ .

(64) We found that the tunneling decay constant ( $\beta$ ) in tunneling junctions of the type  $\text{Ag}^{\text{TS}}\text{-SC}_n\text{CH}_3\text{/Ga}_2\text{O}_3\text{/EGaIn}$  (with  $n = 10, 12, 14, 16$ , or  $18$ ) is  $1.0 \pm 0.12$  per  $\text{CH}_2$ , or  $0.80 \pm 0.10$  Å<sup>-1</sup>. We will discuss the resistivity of the layer of  $\text{Ga}_2\text{O}_3$  and the observed value of  $\beta$  in a separate paper.

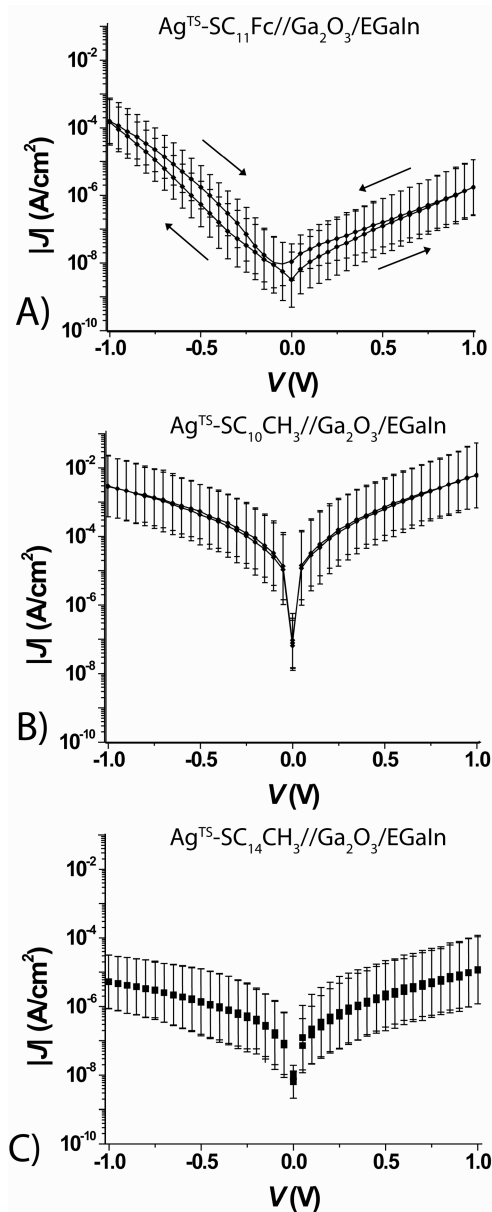


**Figure 4.** Average traces of the absolute value of the current density,  $|J|$ , plotted versus applied voltage for all  $\text{Ag}^{\text{TS}}\text{-SC}_{11}\text{Fc//Ga}_2\text{O}_3/\text{EGaIn}$  junctions (top, 53 junctions, 977 traces,  $0\text{ V} \rightarrow +1\text{ V} \rightarrow -1\text{ V} \rightarrow 0\text{ V}$ ),  $\text{Ag}^{\text{TS}}\text{-SC}_{10}\text{CH}_3//\text{Ga}_2\text{O}_3/\text{EGaIn}$  junctions (middle, 23 junctions, 415 traces,  $0\text{ V} \rightarrow +1\text{ V} \rightarrow -1\text{ V} \rightarrow 0\text{ V}$ ), and of  $\text{Ag}^{\text{TS}}\text{-SC}_{14}\text{CH}_3//\text{Ga}_2\text{O}_3/\text{EGaIn}$  junctions (bottom, 14 junctions, 287 traces,  $0\text{ V} \rightarrow +1\text{ V} \rightarrow -1\text{ V} \rightarrow 0\text{ V}$ ). Each point in each trace represents the value of  $\mu_{\log}$  obtained from the Gaussian fit to the histogram of  $|J|$  at the corresponding voltage, and the error bars are a factor of  $\sigma_{\log}$  above and below this point. Arrows indicate scan direction.

$R$  measured for junctions of  $\text{Ag}^{\text{TS}}\text{-SC}_{11}\text{Fc//Ga}_2\text{O}_3/\text{EGaIn}$  shows both a significant difference from unity as well as a significant difference from both junctions lacking the Fc moiety (even without accounting for the difference in the polarity of rectification between the former and the latter).

We suggest that the small rectification observed in junctions containing  $n$ -alkanethiolates probably results from: (i) the asymmetry of the electrodes (Ag vs  $\text{Ga}_2\text{O}_3/\text{EGaIn}$ ) and/or (ii) the asymmetry of the interfaces between the SAM and the electrodes (covalent vs van der Waals). Ag and EGaIn have similar work functions ( $\Phi_{\text{Ag}}, \Phi_{\text{EGaIn}} \approx 4.5\text{ eV}$ ), but a small difference could cause these junctions to rectify slightly. More

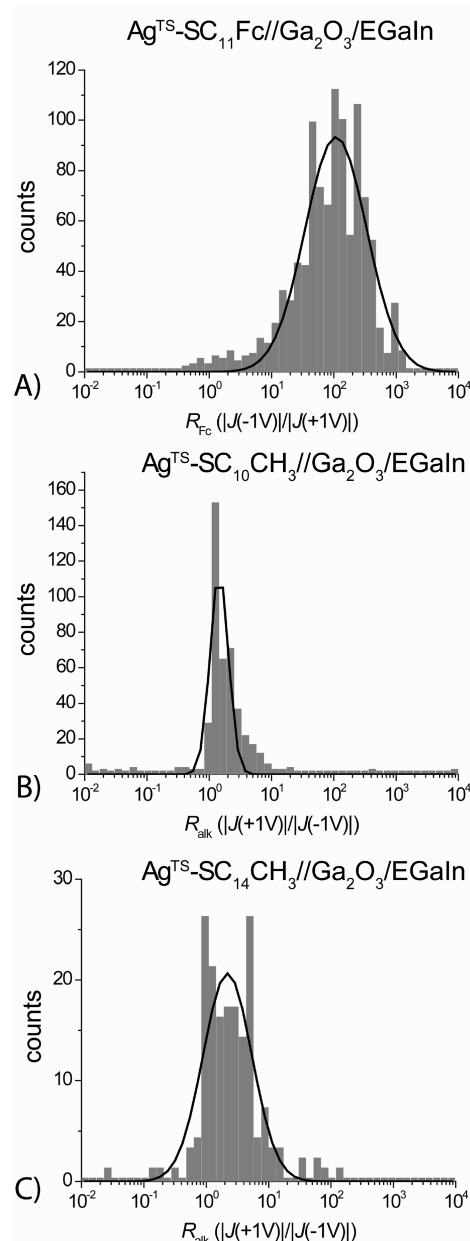


**Figure 5.** Histograms of  $R$  measured at  $\pm 1.0\text{ V}$  for  $\text{Ag}^{\text{TS}}\text{-SC}_{11}\text{Fc//Ga}_2\text{O}_3/\text{EGaIn}$  junctions (53 junctions and 997 traces,  $R = J(-1\text{ V})/J(+1\text{ V})$ ) (A),  $\text{Ag}^{\text{TS}}\text{-SC}_{10}\text{CH}_3//\text{Ga}_2\text{O}_3/\text{EGaIn}$  junctions (17 junctions and 415 traces,  $R = J(+1\text{ V})/J(-1\text{ V})$ ) measured at  $\pm 1.0\text{ V}$ ) (B), and  $\text{Ag}^{\text{TS}}\text{-SC}_{14}\text{CH}_3//\text{Ga}_2\text{O}_3/\text{EGaIn}$  junctions (14 junctions and 287 traces,  $R = J(+1\text{ V})/J(-1\text{ V})$ ) measured at  $\pm 1.0\text{ V}$ ) (C). The solid black lines show the Gaussian fits to these histograms. A fit with  $\mu_{\log} = 1.0 \times 10^2$  and  $\sigma_{\log} = 3.0$  was found in the case of the  $\text{Ag}^{\text{TS}}\text{-SC}_{11}\text{Fc//Ga}_2\text{O}_3/\text{EGaIn}$  junctions. For the  $\text{Ag}^{\text{TS}}\text{-SC}_{10}\text{CH}_3//\text{Ga}_2\text{O}_3/\text{EGaIn}$  junctions and  $\text{Ag}^{\text{TS}}\text{-SC}_{14}\text{CH}_3//\text{Ga}_2\text{O}_3/\text{EGaIn}$  junctions,  $\mu_{\log} = 1.5$  and  $\sigma_{\log} = 1.4$ , and  $\mu_{\log} = 2.1$  and  $\sigma_{\log} = 2.5$ , were determined, respectively.

likely, because the distribution of electron density at the interface between  $\text{Ga}_2\text{O}_3/\text{EGaIn}$  and the SAM is substantially different from the distribution of electron density across the covalent contact between Ag and the SAM, the tunneling barrier seen by charge carriers is asymmetric. Theoretical predictions suggest that rectification ratios on the order of  $\sim 20$  can be achieved with an asymmetric tunneling barrier.<sup>65</sup>

(65) Armstrong, N.; Hoft, R. C.; McDonagh, A.; Cortie, M. B.; Ford, M. J. *Nano Lett.* **2007**, *7*, 3018.

**The Role of the Fc Moiety in Determining the Rectification Ratio.** The  $\text{Ag}^{\text{TS}}\text{-SC}_{11}\text{Fc//Ga}_2\text{O}_3\text{/EGaIn}$  junctions showed a large rectification ratio with higher current at negative bias than positive bias: junctions lacking the Fc moiety, the  $\text{Ag}^{\text{TS}}\text{-SC}_{14}\text{CH}_3\text{/Ga}_2\text{O}_3\text{/EGaIn}$  and the  $\text{Ag}^{\text{TS}}\text{-SC}_{10}\text{CH}_3\text{/Ga}_2\text{O}_3\text{/EGaIn}$  junctions, gave much smaller rectification ratios (by a factor of  $\sim 50$  to  $\sim 100$ ). Using short formation times for the  $\text{SC}_{11}\text{Fc}$  SAMs ( $< 5$  min) decreased the rectification ratio or eliminated rectification ( $R = 1$ ) altogether. Using mixed SAMs of  $\text{HS}(\text{CH}_2)_{10}\text{CH}_3$  and  $\text{HS}(\text{CH}_2)_{11}\text{Fc}$  with increasing ratios of  $\text{HS}(\text{CH}_2)_{10}\text{CH}_3\text{:HS}(\text{CH}_2)_{11}\text{Fc}$  had the same effect. This study will be described in detail in a separate paper.<sup>66</sup> These observations imply an essential role for the Fc moiety, and for ordered (or at least dense) SAMs, in the rectification.

As mentioned above, Zandvliet et al. reported rectification of currents with values of  $R$  of 5–10 in STM-based tunneling junctions incorporating  $\text{SC}_{11}\text{Fc}$ , while we report here a much higher value of  $R$  of  $\sim 30$ – $300$  for SAMs of  $\text{SC}_{11}\text{Fc}$  in our junctions. Possible explanations for this difference could be that: (i) Zandvliet et al. studied SAMs of  $\text{SC}_{11}\text{Fc}$  mixed with  $n$ -alkanethiolates (which seems to lower the rectification ratio), rather than densely packed SAMs of  $\text{SC}_{11}\text{Fc}$  as we did. (ii) The presence of a vacuum gap between the STM tip and the SAM, which is not present in our junctions, could situate the Fc more symmetrically in the junctions.

**The Role of Aging on the Rectification Ratio.** Junctions assembled using aged (1 day old, ambient conditions)  $\text{SC}_{11}\text{Fc}$  SAMs on  $\text{Ag}^{\text{TS}}$  showed only a small  $R$  (close to unity), but with the current amplification at positive voltages. XPS spectra of these aged SAMs on  $\text{Ag}^{\text{TS}}$  showed a large amount of oxygen present, while freshly prepared samples did not have oxygen.

Metzger et al. reported that rectifying junctions with Mg-electrodes, perhaps with magnesium oxide, formed Schottky barriers.<sup>16</sup> Here, we suggest that the formation of  $\text{Ag}_2\text{O}$  on surfaces of  $\text{Ag}^{\text{TS}}$  with SAMs causes the rectification to diminish, and we infer that neither  $\text{Ag}_2\text{O}$  nor  $\text{Ga}_2\text{O}_3$  are responsible, that is, they do not form Schottky barriers, for the large rectification ratios observed in  $\text{Ag}^{\text{TS}}\text{-SC}_{11}\text{Fc//Ga}_2\text{O}_3\text{/EGaIn}$  junctions.

We did not observe a negative differential resistance (NDR) effect. Thus, NDR is not a property of these SAMs.

**The Resistivity of the Layer of  $\text{Ga}_2\text{O}_3$ .** To estimate the resistivity of the layer of  $\text{Ga}_2\text{O}_3$ , we used two copper wires (with diameter of  $80\ \mu\text{m}$  and length 1 cm) to contact, and to measure, the  $J(V)$  characteristics of a drop of EGaIn with its native layer of  $\text{Ga}_2\text{O}_3$  in three different ways. (i) Both copper wires penetrated the surface layer of  $\text{Ga}_2\text{O}_3$ . (ii) One copper wire penetrated the surface layer of  $\text{Ga}_2\text{O}_3$ , and the second wire rested on the layer of  $\text{Ga}_2\text{O}_3$ . (iii) Both copper wires rested on the layer of  $\text{Ga}_2\text{O}_3$ . As a control, we measured the  $J(V)$  curve of one copper wire.

Figure 6 shows that all  $J(V)$  curves are ohmic. We calculated the resistances of the circuits<sup>67</sup> from the slopes of the  $J(V)$  curves. To determine the resistivity of the electronic circuit, we contacted the two copper wires to each other; the resulting circuit had a resistivity of  $\sim 0.0001\ \Omega\ \text{cm}^{-2}$ . The measured resistivity of the bulk EGaIn was  $\sim 0.0006\ \Omega\ \text{cm}^{-2}$  and indicates, as expected, that the bulk EGaIn is highly conductive.

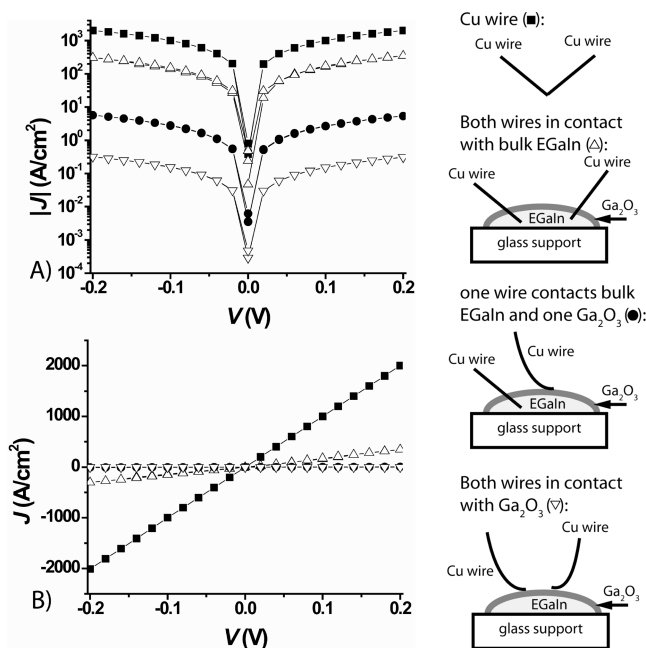


**Figure 6.** The schematic representations show only the copper wires and the  $\text{Ga}_2\text{O}_3\text{/EGaIn}$  of the electronic circuits and the corresponding  $J(V)$  characteristics (semilog plot of the absolute values of  $J$  as a function of potential (A) and the value of  $J$  as a function of potential (B)) with (i) both copper wires in direct contact with each other (■), (ii) both copper wires in contact with bulk EGaIn ( $\Delta$ ), (iii) one copper wire in contact with bulk EGaIn and one copper wire resting at the layer of  $\text{Ga}_2\text{O}_3$  (●), and (iv) both copper wires resting on the layer of  $\text{Ga}_2\text{O}_3$  ( $\nabla$ ).

In our SAM-based tunneling junctions, the needle of the syringe, from which the conically shaped tip of  $\text{Ga}_2\text{O}_3\text{/EGaIn}$  top-electrode is suspended, is in contact with the bulk EGaIn, while the SAM is in contact with the layer of  $\text{Ga}_2\text{O}_3$ . We believe that the  $J(V)$  curve obtained with one copper wire penetrating the layer of  $\text{Ga}_2\text{O}_3$ , and the second copper wire resting on the layer of  $\text{Ga}_2\text{O}_3$ , gives a reasonable value for the resistivity of the layer of  $\text{Ga}_2\text{O}_3$  in our tunneling measurements. The resistivity of this electronic circuit was  $\sim 0.04\ \Omega\ \text{cm}^{-2}$ . Thus, the resistivity was a factor of  $\sim 65$  higher when one wire rested on the layer of  $\text{Ga}_2\text{O}_3$ , and one wire contacted the bulk EGaIn, than when both wires contacted bulk EGaIn. Thus, the layer of  $\text{Ga}_2\text{O}_3$  seems to be significantly more resistive than the bulk EGaIn.

The circuit with both copper wires resting on the layer of  $\text{Ga}_2\text{O}_3$  had a resistivity of  $\sim 0.7\ \Omega\ \text{cm}^{-2}$ . We conclude from this experiment that the copper wires are thin and flexible enough to contact the layer of  $\text{Ga}_2\text{O}_3$  safely without penetration.

The current density at 0.2 V for the  $\text{Ag}^{\text{TS}}\text{-SC}_{10}\text{CH}_3\text{/Ga}_2\text{O}_3\text{/EGaIn}$  junctions is  $2.0 \times 10^{-4}\ \text{A/cm}^2$ . The current density measured at 0.2 V for the circuit with one copper wire contacting the bulk EGaIn and the second wire contacting the layer of  $\text{Ga}_2\text{O}_3$  was  $5.5\ \text{A/cm}^2$ . From this set of experiments, we hypothesize that the layer of  $\text{Ga}_2\text{O}_3$  is resistive, but its resistivity is more than 4 orders of magnitude less than the least resistive SAM, that is,  $\text{SC}_{11}$ , studied in our SAM-based tunneling junctions. More detailed experiments are required to determine the exact influence of the layer of  $\text{Ga}_2\text{O}_3$  on the tunneling characteristics in our SAM-based tunneling junctions.

**The Role of the Layer of  $\text{Ga}_2\text{O}_3$  in the Rectification.** McCreery et al. showed that redox-reactions involving redox-active SAMs and  $\text{TiO}_2$  electrodes caused rectification in their junctions.<sup>17,50,51</sup> These junctions did not rectify currents in the

(66) Reus, W. F.; Nijhuis, C. A.; Whitesides, G. M., unpublished experiments.

(67) The values for the resistance include the resistance of all other components of our circuit: a syringe, a probe to contact the  $\text{Ag}^{\text{TS}}$  surfaces, an electrometer, and wires to connect all components.

absence of the redox-active SAM or  $\text{TiO}_2$ . We performed two experiments to determine if the rectification in  $\text{Ag}^{\text{TS}}\text{-SC}_{11}\text{Fc//Ga}_2\text{O}_3/\text{EGaIn}$  junctions involves redox-reactions between the Fc moieties and the  $\text{Ga}_2\text{O}_3$  oxide layer, or if it is entirely due to the chemical composition of the SAM. (i) We replaced the redox-active SAM, that is,  $\text{SC}_{11}\text{Fc}$ , by a redox-inactive SAM, that is,  $\text{SC}_{11}$  or  $\text{SC}_{15}$ . (ii) We replaced the redox-active  $\text{Ga}_2\text{O}_3/\text{EGaIn}$  top-electrode with a redox-inactive Au top-electrode.

The junctions with a redox-inactive SAM, that is,  $\text{Ag}^{\text{TS}}\text{-SC}_{10}\text{CH}_3/\text{Ga}_2\text{O}_3/\text{EGaIn}$  and  $\text{Ag}^{\text{TS}}\text{-SC}_{14}\text{CH}_3/\text{Ga}_2\text{O}_3/\text{EGaIn}$  rectified currents, as described above, with rectification ratios close to unity (Figures 4 and 5). As concluded earlier, removal of the Fc moiety reduces the rectification ratio by a factor of  $\sim 100$ .

To confirm that the chemical composition of the SAMs in the  $\text{Ag}^{\text{TS}}\text{-SC}_{11}\text{Fc//Ga}_2\text{O}_3/\text{EGaIn}$  junctions causes rectification of currents, and not by the molecule-specific interactions with the layer of  $\text{Ga}_2\text{O}_3$ , or possible redox reactions involving Fc and  $\text{Ga}_2\text{O}_3$ , we fabricated junctions of the type  $\text{Ag}^{\text{TS}}\text{-SC}_{11}\text{Fc//Au}^{\text{TS}}$ . We prepared  $\text{Au}^{\text{TS}}$  top-electrodes by template-stripping Au (with a thickness of 500 nm) from a Si/SiO<sub>2</sub> wafer using Scotch tape (see the Supporting Information for details). The Scotch tape was applied to a layer of gold on a Si/SiO<sub>2</sub> wafer. Removal of the Scotch tape effectively template-stripped the layer of gold from the Si/SiO<sub>2</sub>. Larger areas of gold than defined by the contact area of the Scotch tape could be template-stripped, resulting in a  $\text{Au}^{\text{TS}}$ -foil at the edges of the Scotch tape (Figure S1). We used this thin layer of gold-foil supported on the tape, mounted on a micromanipulator, to contact SAMs of  $\text{SC}_{11}\text{Fc}$  supported on  $\text{Ag}^{\text{TS}}$  bottom-electrode (Figure S1).

Although these junctions were not stable against cycling (we could measure 1–5  $J(V)$  curves for each junction before they shorted), gave low yields of working devices ( $\sim 10\%$ ), and did not generate statistically large numbers of data (five junctions out of 40 rectified currents; the remaining junctions shorted), they yielded qualitatively confirming data. The  $\text{Ag}^{\text{TS}}\text{-SC}_{11}\text{Fc//Au}^{\text{TS}}$  junctions rectified currents with rectification ratios of  $\sim 10$ – $100$  and showed  $J(V)$  characteristics similar to those obtained with  $\text{Ag}^{\text{TS}}\text{-SC}_{11}\text{Fc//Ga}_2\text{O}_3/\text{EGaIn}$  junctions (Figure S2). Thus, unlike the tunneling junctions reported by McCreery et al., where both a redox-active SAM and a redox-active  $\text{TiO}_2$  top-electrode were required for rectification,<sup>17,50,51</sup> using a junction without the possible redox-active layer of  $\text{Ga}_2\text{O}_3$  did not diminish rectification of currents in tunneling junctions with redox-active SAMs of  $\text{SC}_{11}\text{Fc}$ . This experiment argues strongly that the rectification of currents by  $\text{Ag}^{\text{TS}}\text{-SC}_{11}\text{Fc//Ga}_2\text{O}_3/\text{EGaIn}$  junctions is caused by the chemical structure of the SAM inside the junctions, rather than by specific Fc// $\text{Ga}_2\text{O}_3/\text{EGaIn}$  interfacial effects, or by redox reactions involving Fc and  $\text{Ga}_2\text{O}_3$ .

As mentioned earlier, junctions with molecules of  $\text{SC}_{11}\text{Fc}$  on Au and a STM top-electrode rectified currents with rectification ratios of  $\sim 5$ – $10$ .<sup>46</sup> The fact that rectification has been observed in three different types of tunneling junctions ( $\text{Ag}^{\text{TS}}\text{-SC}_{11}\text{Fc//Ga}_2\text{O}_3/\text{EGaIn}$ ,  $\text{Ag}^{\text{TS}}\text{-SC}_{11}\text{Fc//Au}^{\text{TS}}$ , and Au- $\text{SC}_{11}\text{Fc}$  contacted with an STM tip) with the same molecule in the SAM, (i.e.,  $\text{SC}_{11}\text{Fc}$ ) indicates that the rectification of currents is induced by the structure of the molecules inside the tunneling junctions, rather than by other differences of the junctions (e.g., different electrode materials, the redox properties of the  $\text{Ga}_2\text{O}_3$  film, or different types of contact between the electrodes and  $\text{CH}_3$  or Fc groups).

**Stability of the Junctions.** In the set used for statistical analysis, of the 50  $\text{Ag}^{\text{TS}}\text{-SC}_{11}\text{Fc//Ga}_2\text{O}_3/\text{EGaIn}$  junctions that rectified on the first trace, 46 were still rectifying after 20 traces

(28 min of measurement time). To test the stability of these junctions further, we carried out measurements beyond the typical 21  $J(V)$  traces. We chose arbitrary limits of 100 traces and 200 traces over which to measure four junctions and one junction, respectively (these junctions were not included in the set of 53 junctions we used for statistical analysis).

Figure 7 shows the results obtained for two of these junctions. In general, the first one to five traces on each junction were noisy, after which the current density and  $R$  stabilized. Junction 1 shows noisy behavior at scan number 72 due to mechanical vibrations (Figure 7A and B) of the measuring apparatus.<sup>68</sup> Junction 2 shows a gradual decrease in  $R$ , perhaps due to mechanical drift of the micromanipulator, or chemical degradation of the Fc moieties during measurement (Figure 7C and D). We generally observed a slight decrease of current density over many consecutive traces, probably due to chemical degradation of the Fc-moieties upon repeated cycling of potential. One junction shorted and ceased to rectify after 90 traces (perhaps due to mechanical vibrations), but the remaining four continued to rectify through all 100 or 200 traces, as applicable. While we cannot quantify the longevity of these junctions, we conclude that they are stable for 100 or more traces.

In all  $J(V)$  measurements of the  $\text{Ag}^{\text{TS}}\text{-SC}_{11}\text{Fc//Ga}_2\text{O}_3/\text{EGaIn}$  junctions, we observed a small current ( $\sim 10^{-9}$ – $10^{-8}$  A/cm<sup>2</sup>; Figure 8) near  $V = 0$  V due to either (i) capacitive charging, (ii) an electrochemical process, for example, oxidation and reduction processes of the Fc moieties, or (iii) conformational rearrangements of the SAM, an effect which we do not observe, or which is too small to observe, in junctions of alkanethiolates (see Figure 4). This small current near zero bias varies (by 1 order of magnitude) from measurement to measurement, but is always very small. Figure 8A shows, on a linear scale, one representative  $J(V)$  curve, that is, a trace with  $J(V)$  characteristics within one log-standard deviation of the log-mean value of  $J$  for the entire data set, of a  $\text{Ag}^{\text{TS}}\text{-SC}_{11}\text{Fc//Ga}_2\text{O}_3/\text{EGaIn}$  junction measured at  $\pm 1.0$  V. Figure 8B shows the same  $J(V)$  curve as in Figure 8A at potentials between  $-0.5$  and  $0.5$  V. We normally report the absolute values of  $|J|$  on a logarithmic scale, as in Figure 8C, which shows the same data as Figure 8A on a semilog plot. The small current near zero bias discussed above causes the semilog plots to appear to have anomalies close to the origin (Figure 8C).

**Mechanism of Rectification.** We will discuss the mechanism of rectification in a separate paper.<sup>69</sup> Here, we give a brief discussion about the mechanism of rectification in the  $\text{Ag}^{\text{TS}}\text{-SC}_{11}\text{Fc//Ga}_2\text{O}_3/\text{EGaIn}$  junctions.

The groups of Baranger et al.<sup>39</sup> and Kornilovitch et al.<sup>40</sup> have proposed that an asymmetrically positioned molecular orbital (either HOMO or LUMO) inside a tunneling junction can rectify current. We believe that our molecular rectifier operates according to a mechanism that is similar to that proposed by these groups.

In the  $\text{Ag}^{\text{TS}}\text{-SC}_{11}\text{Fc//Ga}_2\text{O}_3/\text{EGaIn}$  junctions, the Fc group forms a van der Waals contact with the  $\text{Ga}_2\text{O}_3/\text{EGaIn}$ , but is separated from the  $\text{Ag}^{\text{TS}}$  bottom-electrode by the  $\text{C}_{11}$  alkyl

(68) Our setup is not completely vibration free. Vibration caused some of the junctions to fail during data collection. A small tick on the Faraday cage, in which our setup is installed, during data collection caused the junctions to short.

(69) A detailed physical-organic study to control the potential drops along the SAM, including  $J(V)$  curves measured at different temperatures, to elucidate the mechanism of rectification in more detail, will be reported in a separate paper: Nijhuis, C. A.; Reus, W. F.; Whitesides, G. M., manuscript in preparation.

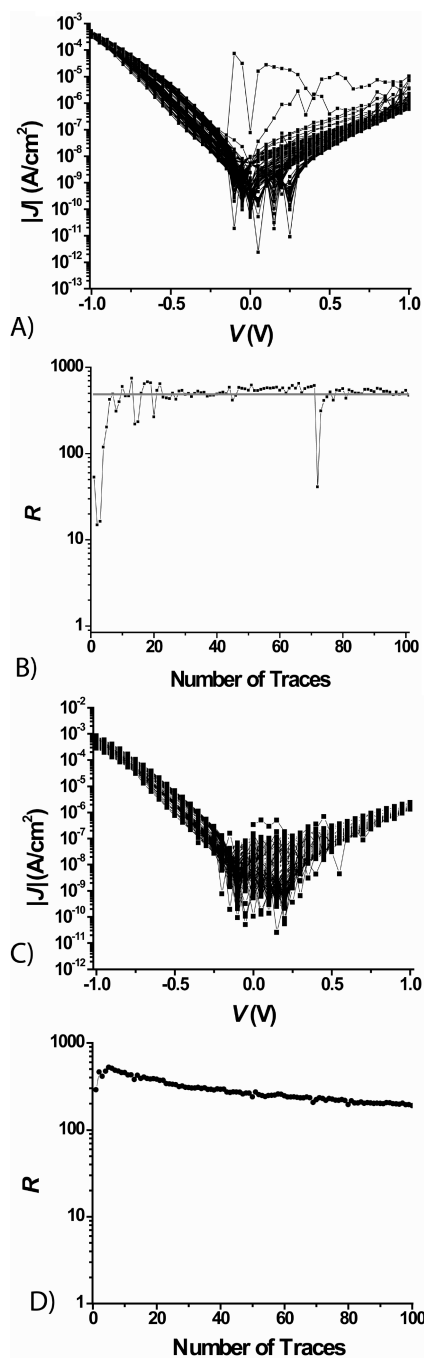


**Figure 7.** Stability measurements of two  $\text{Ag}^{\text{TS}}\text{-SC}_{11}\text{Fc//Ga}_2\text{O}_3/\text{EGaIn}$  junctions. A total of 100  $J(V)$  traces from each of two different  $\text{Ag}^{\text{TS}}\text{-SC}_{11}\text{Fc//Ga}_2\text{O}_3/\text{EGaIn}$  junctions are shown in (A) (junction 1) and (C) (junction 2). The corresponding plot of  $\log(R)$  versus number of traces for junctions 1 (B) and 2 (D), showing that  $R$  becomes stable after the first few traces and continues to stabilize, remaining roughly constant from traces 25–100. The gray line in (B) indicates the average  $R$  for junction 1 ( $R = 487$ ). ■ = data point and the lines are a guide to the eye.

chain. The HOMO level of the Fc is thus close to and coupled with the orbitals of the  $\text{Ga}_2\text{O}_3/\text{EGaIn}$  system. Figure 9 sketches the energy level diagram of the  $\text{Ag}^{\text{TS}}\text{-SC}_{11}\text{Fc//Ga}_2\text{O}_3/\text{EGaIn}$  junctions. The HOMO level of the Fc is  $-5.0$  eV (estimated from cyclic voltammetry, Figure 2) and is lower than the Fermi levels of Ag ( $-4.7$  eV) and EGaIn ( $-4.3$  eV). In our experiments, we biased the  $\text{Ga}_2\text{O}_3/\text{EGaIn}$  top-electrode

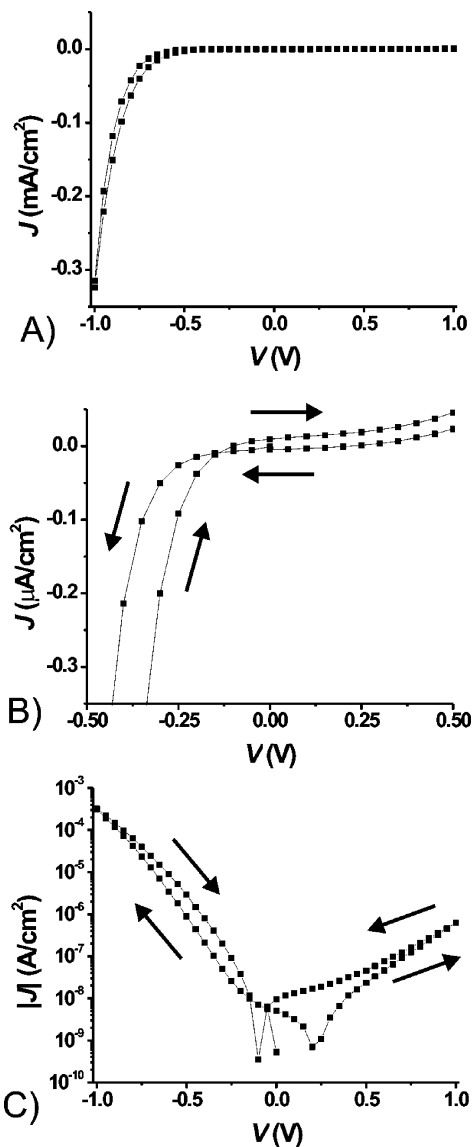


**Figure 8.**  $J(V)$  curve of a  $\text{Ag}^{\text{TS}}\text{-SC}_{11}\text{Fc//Ga}_2\text{O}_3/\text{EGaIn}$  junction measured between  $\pm 1.0$  V (A) and an expanded section (B) clearly showing a non-zero current at zero bias. In (C), the corresponding  $|J|(V)$  curve is shown. The arrows indicate the scan direction.

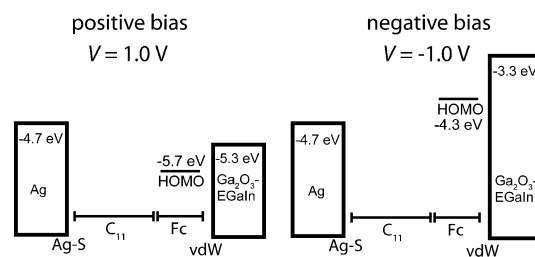


**Figure 9.** Proposed schematic energy level diagram for  $\text{Ag}^{\text{TS}}\text{-SC}_{11}\text{Fc//Ga}_2\text{O}_3/\text{EGaIn}$  junctions at 1.0 V (left) and  $-1.0$  V (right), Fc = ferrocene, vdW = van der Waals interface, Ag–S = the silver–thiolate interface,  $\text{C}_{11}$  = the alkyl chain.

and connected the  $\text{Ag}^{\text{TS}}$  bottom-electrode to the ground. The HOMO level of the Fc group follows the potential of the  $\text{Ga}_2\text{O}_3/\text{EGaIn}$  top-electrode, because most of the potential drops across the  $\text{C}_{11}$  alkyl chain. The HOMO level of the Fc group can only participate in charge transport when it

overlaps with the Fermi levels of the top- or bottom-electrodes. At negative bias, the Fermi level of the Ga<sub>2</sub>O<sub>3</sub>/EGaIn top-electrode increases and so does the HOMO of the Fc group. Consequently, the HOMO of the Fc group can participate in charge transport when it overlaps with the Fermi levels of the electrodes. At positive bias, however, the Fermi level of the top-electrode decreases and so does the HOMO level of the Fc group. In the applied bias window, the HOMO level of the Fc group cannot participate in charge transport. Thus, rectification occurs because the HOMO of the Fc group is involved in charge transport only at negative bias.

The layer of Ga<sub>2</sub>O<sub>3</sub> may lower the values of  $J$ , but it does not influence the relative potential drops across the SAMs inside the tunneling junctions. The rectification ratio is the ratio of current densities across the same junctions (eq 1) measured at opposite bias ( $\pm 1.0$  V). Thus, the resistivity of the layer of Ga<sub>2</sub>O<sub>3</sub> does not contribute to the value of  $R$ .

## Conclusions

**The Fc Groups of the Ag<sup>TS</sup> Electrodes Are Densely Packed.** SAMs incorporating Fc-terminated molecules, and diluted with alkanethiolates, show ideal (that is, symmetrical) cyclic voltammograms, while densely packed Fc SAMs show peak broadening and two or more redox events.<sup>53,54,56,57</sup> The different oxidation and reduction waves in the cyclic voltammograms correspond to Fc moieties in a different environment. When Fc SAMs are diluted with alkanethiolates, (nearly) all Fc moieties are isolated (in an electrochemical sense) and will be in the same environment (except in regions containing defects). In the case of densely packed, Fc-terminated SAMs, neighboring effects can dominate: a Fc moiety that is oxidized will influence the oxidation potentials of its neighbors. Thus, the shape of a cyclic voltammogram can be used to estimate the quality of the Fc SAM. We used cyclic voltammetry to calculate the surface coverage of the Fc moieties, to estimate the energy of the HOMO, and to gauge the quality of the Fc-terminated SAM. In the systems we used to study tunneling and rectification, cyclic voltammetry showed that the Fc moieties interact strongly with one another and suggested that the SAMs were densely packed.

**Junctions with Composition Ag<sup>TS</sup>-SC<sub>11</sub>Fc//Ga<sub>2</sub>O<sub>3</sub>/EGaIn Are Strongly Rectifying ( $R = 1.0 \times 10^2$ ).** The value of  $R = 1.0 \times 10^2$  (3.0) we report for the Ag<sup>TS</sup>-SC<sub>11</sub>Fc//Ga<sub>2</sub>O<sub>3</sub>/EGaIn junctions is larger than most values of rectification reported in the literature ( $R = 1 - 10$ , with no uncertainty reported). The stability, reproducibility, and magnitude of  $R$  in these junctions make this system suitable for conducting physical-organic studies to determine the mechanism of rectification; such experiments are currently underway in our laboratories.

**Statistical Analysis of the Rectification Ratio Requires Hundreds of Data To Establish Significance.** Statistical analysis of the rectification ratio of a large number of junctions and traces is a prerequisite to claiming rectification and quantifying its magnitude and reproducibility. We found a log-normal distribution of the rectification ratio, explained as follows. The rectification ratio was determined by the ratio of current densities of 997 traces at  $\pm 1.0$  V. Because the current densities are exponentially dependent on the distance between the top- and bottom-electrodes,<sup>4,17</sup> and because the effective distance between the top- and bottom-electrodes is plausibly distributed

normally, the current densities and the rectification ratio determined from the current densities are both log-normally distributed.

**The Ga<sub>2</sub>O<sub>3</sub>/EGaIn Top-Electrodes Are Useful To Form SAM-Based Tunneling Junctions, But Have Disadvantages as Well as Advantages.** The use of Ga<sub>2</sub>O<sub>3</sub>/EGaIn top-electrodes to contact SAMs does not rely on metal evaporation, is nontoxic, and does not damage the molecules of the SAMs. These properties make this methodology especially attractive for studying charge transport through metal-SAM-metal oxide-metal junctions. The use of Ga<sub>2</sub>O<sub>3</sub>/EGaIn as top-electrodes eliminates many of the problems associated with top-contacts of Hg. This use (i) generates junctions that are more stable than those of Hg, (ii) does not require a solvent bath with the resulting complexities of solvent thin films and intercalating the SAM, and (iii) permits the investigation of single monolayer junctions (i.e., with contacts deposited directly on the SAM), while Hg junctions only make it possible to study double monolayer junctions.

Although Ga<sub>2</sub>O<sub>3</sub>/EGaIn is an attractive system, it still has disadvantages and uncertainties. (i) We cannot define the thickness of the layer of Ga<sub>2</sub>O<sub>3</sub> and suspect it changes during the course of a set of experiments with a single tip. The thickness of the layer of Ga<sub>2</sub>O<sub>3</sub> grown under a controlled atmosphere of O<sub>2</sub> is 0.5–1.0 nm,<sup>33</sup> but is probably thicker in our junctions due to mechanical deformation, fracture, and reformation on the conically shaped Ga<sub>2</sub>O<sub>3</sub>/EGaIn top-electrode. (ii) We do not know the conductivity of the layer of Ga<sub>2</sub>O<sub>3</sub> in the junctions, but believe it is greater than that of the SAM by at least 4 orders of magnitude. We estimated the resistance of the layer of Ga<sub>2</sub>O<sub>3</sub> by measuring the  $J(V)$  characteristics of EGaIn with its layer of Ga<sub>2</sub>O<sub>3</sub> by contacting the layer of Ga<sub>2</sub>O<sub>3</sub> and the bulk EGaIn with two thin copper wires. The current density (measured at 0.2 V) for this circuit was 4 orders of magnitude larger than that of the Ag<sup>TS</sup>-SC<sub>10</sub>CH<sub>3</sub>//Ga<sub>2</sub>O<sub>3</sub>/EGaIn junctions. (iii) The SAM//Ga<sub>2</sub>O<sub>3</sub> interface is ill-defined topographically. We believe that the Ga<sub>2</sub>O<sub>3</sub> forms a van der Waals contact with the SAMs. (iv) The contact area of the Ga<sub>2</sub>O<sub>3</sub> with the SAM is correspondingly ill-defined. The measured contact areas of the Ga<sub>2</sub>O<sub>3</sub>/EGaIn top-electrode with the SAMs were 100–300  $\mu\text{m}^2$ . Probably the Ga<sub>2</sub>O<sub>3</sub> forms conformal contacts over small areas (nm scale) but not uniformly over large areas ( $\mu\text{m}$  scale); regions that are not in contact will result in an overestimation of the actual contact area and an underestimation of  $J$ .<sup>35</sup>

**The Influence of the Layer of Ga<sub>2</sub>O<sub>3</sub> on the Value of the Rectification Ratio Is Negligible.** The uncertainties in the resistance of the layer of Ga<sub>2</sub>O<sub>3</sub>, and in the estimate of the real contact area of the Ga<sub>2</sub>O<sub>3</sub>/EGaIn with the SAM, will influence the measured current densities. The resistance and thickness of the Ga<sub>2</sub>O<sub>3</sub> layer may vary from experiment to experiment and may partially explain the distribution of the observed current densities. Rectification seems especially attractive as a parameter to use in studying the mechanism of charge transport across SAM-based tunneling junctions, because the rectification ratio is the ratio of the absolute currents across the same junction at opposite bias (eq 1). Thus, measuring the rectification ratio compensates for random variations in the current density due to changes in contact area and resistance among different junctions. Measuring rectification thus minimized the contribution of the layer of Ga<sub>2</sub>O<sub>3</sub> layer, and its associated resistance, to the measured charge transport properties of the SAM.

**The Rectification in  $\text{Ag}^{\text{TS}}\text{-SC}_{11}\text{Fc//Ga}_2\text{O}_3/\text{EGaIn}$  Junctions Is a Molecular Effect.** We believe that the rectification observed in the  $\text{Ag}^{\text{TS}}\text{-SC}_{11}\text{Fc//Ga}_2\text{O}_3/\text{EGaIn}$  junctions is due to the molecular properties of the  $\text{SC}_{11}\text{Fc}$  SAM and is not caused by redox reactions involving metal oxides with the redox-active SAMs,<sup>17,50,51</sup> or other interface effects,<sup>16,17</sup> for two reasons. (i) Junctions without the Fc moiety, that is, comprising SAMs of  $\text{SC}_{10}\text{CH}_3$  and  $\text{SC}_{14}\text{CH}_3$ , show only a small rectification close to unity ( $R = 1\text{--}5$ ). These junctions were measured under the same conditions as the  $\text{SC}_{11}\text{Fc}$  junctions. For this reason, the large rectification observed in  $\text{Ag}^{\text{TS}}\text{-SC}_{11}\text{Fc//Ga}_2\text{O}_3/\text{EGaIn}$  junctions cannot be caused by redox behavior of silver oxide or gallium oxide, or by any inherent electronic asymmetries in the junctions, such as differences in the electrodes (the Ag bottom-electrode and  $\text{Ga}_2\text{O}_3/\text{EGaIn}$  top-electrode) or in the contacts to the SAM (covalent contact of the SAM with the Ag bottom-electrode, and van der Waals contact with the  $\text{Ga}_2\text{O}_3/\text{EGaIn}$  top-electrode). Rather, the Fc moiety itself is the most likely origin of the rectification. (ii) Junctions of  $\text{SC}_{11}\text{Fc}$  with top-electrodes other than  $\text{Ga}_2\text{O}_3/\text{EGaIn}$ , that is, a tungsten STM-tip or  $\text{Au}^{\text{TS}}$ , also rectified currents. Zandvliet et al. reported a STM study of SAMs of  $\text{SC}_n\text{Fc}$  (with  $n = 3, 5,$  and  $11$ ) on Au (using a tungsten STM-tip) that rectified currents while SAMs of  $\text{SC}_{n-1}\text{CH}_3$  (with  $n = 8$  or  $12$ ) with the same experimental conditions did not.<sup>46</sup> These authors did not discuss the mechanism of rectification.

Junctions of the form  $\text{Ag}^{\text{TS}}\text{-SC}_{11}\text{Fc//Au}^{\text{TS}}$  produced  $J(V)$  curves similar to those obtained with junctions of  $\text{Ag}^{\text{TS}}\text{-SC}_{11}\text{Fc//Ga}_2\text{O}_3/\text{EGaIn}$  and rectified currents with rectification ratios of 10–100 (see the Supporting Information for details). These junctions do not contain a layer of gallium oxides, and the work function of Au (5.1 eV) is close to that of Ag (4.7 eV). The fact that rectification has been observed for the same chemical system in different types of tunneling junctions supports our conclusion that rectification in tunneling junctions incorporating SAMs with Fc termini is a molecular effect. Currently, we are investigating the mechanism of this phenomenon.<sup>69</sup>

**Acknowledgment.** The Netherlands Organization for Scientific Research (NWO) is kindly acknowledged for the Rubicon grant (C.A.N.) supporting this research. Prof. Jurriaan Huskens of the University of Twente is acknowledged for allowing us to perform the electrochemical measurements in his group. We acknowledge the NSF (grant CHE-05180055) for funding.

**Supporting Information Available:** Nomenclature; details of the statistical analysis; experimental details; and  $I(V)$  curves and optical micrographs of  $\text{Ag}^{\text{TS}}\text{-SC}_{11}\text{Fc//Au}^{\text{TS}}$  junctions. This material is available free of charge via the Internet at <http://pubs.acs.org>.

JA9048898